Article

Energy state guides reward seeking via an extended amygdala to lateral hypothalamus pathway

Kuldeep Shrivastava[1], Vikshar Athreya[1], Yi Lu[1], Jorge Luis-Islas[1], Ashley Han[1], Tess F. Kowalski[1] & Mark A. Rossi [1,2,3,4] ✉

Impaired regulation of food intake underlies numerous health problems, including obesity and type 2 diabetes, yet how brain systems controlling reward seeking become dysregulated to promote overeating is unknown. Glutamatergic neurons of the lateral hypothalamic area (LHA) are thought to act as a brake on feeding, which is dysregulated during diet-induced obesity. These neurons receive input from the extended amygdala, including the bed nucleus of the stria terminalis (BNST). However, the circuit mechanisms underlying the ability of this pathway to control feeding behavior and how they contribute to dysregulated eating are unclear. Here, we discover that BNST projections to LHA (BNST→LHA) promote reward seeking in an energy state-dependent manner by combining optogenetics, in vivo multiphoton calcium imaging, and electrophysiology in mice. Synaptic strength and neuronal function within the BNST→LHA pathway are dynamically regulated according to energy state to guide reward seeking. These findings suggest that hormonal factors modulate the function of the BNST→LHA pathway to align food seeking with current energy needs.

The increasing prevalence of obesity is a significant global public health concern[1,2]. Eating behavior is coordinated by distributed brain circuitry that adjusts food seeking and consumption based on changing energy demands. Dysfunction within this circuitry is thought to underlie pathological eating, which can lead to the development of obesity and type 2 diabetes[3–6]. However, the neurocircuit mechanisms controlling feeding behavior and how they contribute to aberrant food seeking remain poorly characterized.

The lateral hypothalamic area (LHA) is a critical neuroanatomical substrate that regulates diverse motivated behaviors, including all major aspects of eating[4,7–12]. Early experiments demonstrated that lesioning the LHA abolishes feeding, whereas electrical or chemical stimulation promotes food approach and consumption[12–16]. Recent experiments have revealed that the LHA comprises functionally distinct cell types and with unique synaptic inputs[4,17–23]. Among these cell types, those expressing the vesicular glutamate transporter 2 (Vglut2, encoded by *Slc17a6*) are thought to suppress feeding behavior[21,24–28]. LHA[Vglut2] neuron activation halts feeding, and prolonged exposure to obesogenic food causes widespread transcriptional and functional remodeling within this population[21]. The circuit mechanisms contributing to LHA[Vglut2] neuron function as well as how these circuits adapt to changing energy demands remain elusive.

LHA[Vglut2] neurons receive monosynaptic input from inhibitory GABAergic neurons residing in the bed nucleus of the stria terminalis (BNST)[24]. The BNST is a component of the extended amygdala and is generally thought to mediate stress, anxiety, and arousal[29,30]. In addition to these functions, BNST projections to the LHA (BNST→LHA) have recently been shown to influence distinct aspects of motivated

[1]Center for NeuroMetabolism, Child Health Institute of New Jersey, Rutgers Robert Wood Johnson Medical School, New Brunswick, NJ 08901, USA. [2]Department of Neuroscience and Cell Biology, Rutgers Robert Wood Johnson Medical School, New Brunswick, NJ 08901, USA. [3]Department of Psychiatry, Rutgers Robert Wood Johnson Medical School, New Brunswick, NJ 08901, USA. [4]Brain Health Institute, Rutgers University, New Brunswick, NJ 08901, USA. ✉e-mail: Mark.Rossi@rutgers.edu

behavior including food seeking and consumption[24,31,32]. The BNST comprises primarily GABAergic neurons, which are activated by food consumption[33–35]. A subset of these BNST neurons have been shown to project to the LHA, where they are thought to promote feeding through direct inhibition of LHA^{Vglut2} neurons[24]. Thus, while the importance of the BNST→LHA pathway for feeding behavior has been recognized, the circuit and synaptic mechanisms underlying these functions remain to be determined.

In this study, we investigated the role of the BNST→LHA^{Vglut2} pathway in reward seeking behavior. Using optogenetic manipulations combined with in vivo deep brain calcium imaging, we demonstrate that BNST→LHA stimulation induces reward seeking via inhibition of LHA^{Vglut2} neurons. The magnitude of this behavioral response depends on current energy needs. Fasting causes increased behavioral sensitivity to BNST→LHA stimulation, which is mediated by changing synaptic strength within the BNST→LHA^{Vglut2} pathway. Moreover, we have also found that overfeeding with an obesogenic diet transiently blunts such state-dependent behavioral sensitization and LHA^{Vglut2} neuron inhibition. This circuit remodeling can be rescued by returning mice to a low-calorie diet. Finally, we demonstrate that LHA^{Vglut2} neurons are necessary for BNST→LHA induced reward seeking, which is bidirectionally controlled by hunger and satiety hormones. Collectively, these results reveal an energy state-dependent control mechanism for reward seeking that becomes dysregulated by overnutrition.

Results

Stimulation of BNST projections to LHA induces state-dependent reward seeking

Acute stimulation of the inhibitory projections from the BNST to the LHA induces food approach and consumption in freely moving mice[24,36]. To test whether activation of the BNST→LHA pathway induces seeking behavior even when food is not immediately available, we performed optogenetic stimulation of BNST axons within the LHA during a sucrose consumption task. AAV-Syn-ChR2-eYFP or the control vector AAV-Syn-eYFP were injected into the BNST, and optical fibers were implanted above the LHA (Fig. 1A, B and Fig. S1). In brain slice recordings, blue light reliably elicited action potentials in BNST neurons at frequencies up to 40 Hz (Fig. 1C, D). To test whether BNST→LHA activation promotes reward seeking, headfixed mice consumed randomly delivered drops of 10% sucrose solution from a delivery spout positioned directly in front of them. On 50% of trials, BNST→LHA axons were stimulated with 473-nm light pulses (5–40 Hz, pseudorandomized across sessions) during the 3 s immediately preceding sucrose availability while licks at the delivery spout were monitored (Fig. 1E). Importantly, no external cues indicated sucrose availability prior to its delivery. We observed a frequency-dependent increase in the rate of licking (a measure of sucrose seeking) and a reduction in the latency to initiate licking during stimulation in the ChR2 group that was not observed in eYFP controls (Fig. 1F–J). Interestingly, the ability of BNST→LHA stimulation to evoke sucrose seeking depended on the mouse's energy state. When mice were ad libitum fed, evoked sucrose seeking was modest at low stimulation frequencies. However, following an overnight fast, sensitivity to low-frequency stimulation was increased (Fig. 1F–H). eYFP controls showed no effect of laser stimulation (Fig. 1I, J and S1B). Potentiated sucrose seeking prior to availability was absent for both groups during trials in which stimulation was not delivered (Fig. S1D). Together, these results indicate that fasting sensitizes mice to BNST→LHA stimulation induced reward seeking.

Because stimulation of GABAergic BNST projections to the LHA has previously been shown to induce feeding when food is available, we next asked whether licking was potentiated if the BNST→LHA pathway was stimulated while sucrose was available. Interestingly, consummatory licking was not increased in ad libitum fed ChR2 mice

relative to eYFP controls when stimulation coincided with sucrose availability (Fig. S2A–B). This result suggests that BNST→LHA stimulation induces goal-directed seeking behavior that is absent when the goal (i.e., sucrose consumption) is achieved. To further test this possibility, we next asked whether BNST→LHA activation is sufficient to promote intake of an unpalatable tastant. Sucrose trials were randomly interspersed with trials in which drops of the bitter tastant quinine (1.5 mM) were delivered. BNST→LHA stimulation was not sufficient to induce the consumption of quinine above control levels even when motivation was increased by fasting or dehydration (Fig. S2C–F). Together, these results confirm that licking evoked by BNST→LHA stimulation is indeed goal-directed.

BNST^{Vgat} neurons projecting to LHA are active during consumption and sensitive to satiety state

Based on the observation that mice were more sensitive to BNST→LHA stimulation after fasting, we hypothesized that fasting increases excitability in BNST→LHA neurons. To test this possibility, we recorded excitability in LHA-projecting BNST neurons. A retrogradely trafficked virus encoding eYFP (retroAAV-Syn-eYFP) was injected into the LHA of wild-type mice. Approximately three weeks later, whole-cell patch clamp recordings were made from eYFP-expressing BNST neurons (Fig. 2A and S3A). BNST→LHA neurons were more excitable during fasting. BNST→LHA neurons fired more action potentials in response to injections of positive current but did not exhibit altered basal firing rates after an overnight fast (Fig. 2B, C, S3B, C).

To test whether enhanced BNST→LHA neuronal excitability is functionally relevant for reward seeking behavior, we next recorded activity within this pathway during reward consumption in vivo. Since the BNST→LHA pathway is largely GABAergic[24,37], we expressed the genetically encoded calcium indicator, GCaMP, in these neurons using an intersectional viral strategy[26,38] (Fig. 2D). Vgat-Cre mice were injected with a virus encoding a retrogradely trafficked flippase (retroAAV-mCherry-FlpO) in the LHA and Cre-on/Flp-on-GCaMP6m in BNST. A microendoscopic lens was then implanted above the BNST, yielding optical access to BNST^{Vgat}→LHA neurons (Fig. 2E–G and S3D, E). BNST^{Vgat}→LHA calcium dynamics were monitored during sucrose consumption in fed and fasted states (Fig. 2H and S3F). When mice were ad libitum fed, BNST^{Vgat}→LHA neurons were largely unresponsive during sucrose consumption (1/54; 2% excited); however, after an overnight fast, many cells were excited (12/53; 22% excited) when mice initiated a bout of sucrose consumption. The amplitude of the calcium response and the number of responsive neurons were significantly increased following an overnight fast (Fig. 2H–J). We tracked the activity of a subset of individual neurons across both fed and fasted recordings, which also exhibited stronger responses to sucrose consumption when fasted compared to when mice were ad libitum fed (Fig. 2K and S3G–I). We next asked whether the observed increased responsivity to sucrose rewards was specific to fasting and sucrose or whether BNST^{Vgat}→LHA neurons showed general motivational modulation of responding. Neurons were generally less responsive to consumption of the non-caloric sweetener saccharine compared to sucrose (Fig. S3J) and showed state-dependent responding to water rewards such that they responded most strongly to water when mice were dehydrated (Fig. S3K). Together, these results demonstrate that BNST^{Vgat}→LHA neurons are more responsive to caloric sucrose rewards when fasted. This effect is likely mediated by increased neuronal excitability within this pathway and is consistent with the increased behavioral sensitivity to BNST→LHA stimulation observed after fasting.

Fasting enhances inhibitory tone within the BNST→LHA^{Vglut2} pathway

Since BNST^{Vgat} neurons preferentially synapse onto Vglut2 neurons within the LHA[24], we next tested whether synaptic strength in this pathway is altered by fasting (Fig. 3). Vglut2-Cre mice were injected
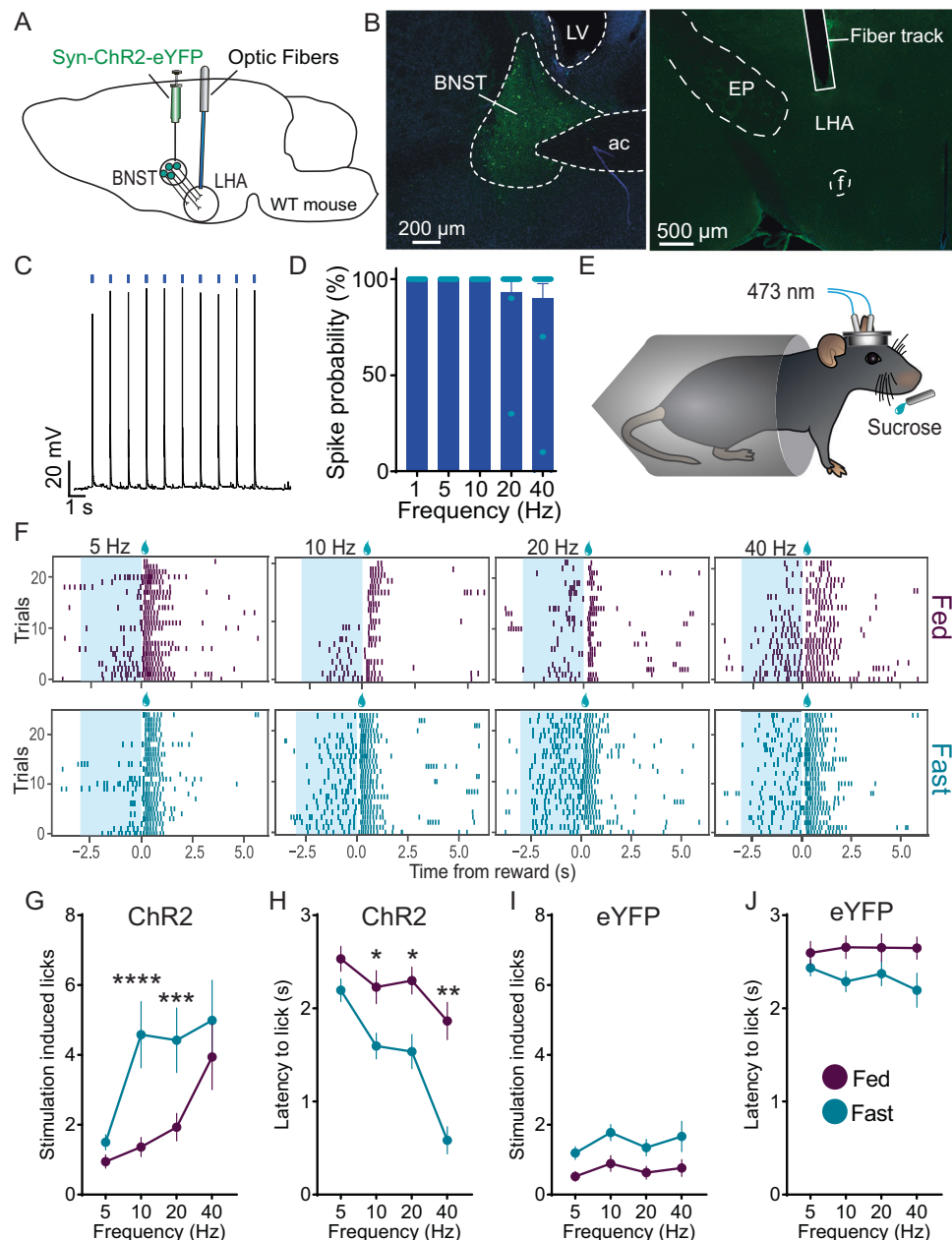
Fig. 1 | Stimulation of BNST projections to LHA evokes energy state-dependent reward seeking. A Experimental schematic. AAV-syn-ChR2-eYFP was injected in BNST and optical fibers were implanted bilaterally above the LHA in WT mice. **B** Histological validation depicting ChR2-eYFP expression in BNST and optic fiber placement above the LHA. ac anterior commissure, EP entopeduncular nucleus, f fornix, LV lateral ventricle. **C** Example whole-cell current clamp recording from a ChR2-expressing BNST neuron. Light pulses (blue) reliably evoked action potentials. **D** Probability of spiking in response to pulse trains of blue light ($n = 12$ neurons). **E** Schematic of experimental design for optogenetic stimulation in head-fixed mice. **F** Raster plots of licking during fed and fasted conditions across a range of stimulation frequencies. Stimulation was delivered during blue shaded region. **G** Licking during the stimulation period increased with fasting for the ChR2 group (two-way ANOVA: main effect of Satiety: $F_{(1,11)} = 9.08$, $p = 0.01$; main

effect of Frequency: $F_{(3,33)} = 8.54$, $p = 0.0002$; Interaction: $F_{(3,33)} = 4.44$, $p = 0.01$. **H** Latency to lick from onset of stimulation for ChR2 group (two-way ANOVA: main effect of Satiety: $F_{(1,11)} = 18.74$, $p = 0.001$; main effect of Frequency: $F_{(3,33)} = 26.94$, $p = 5.36 \times 10^{-9}$; Interaction: $F_{(3,33)} = 6.072$, $p = 0.002$). **I** Stimulation had no effect on licking in eYFP controls (two-way ANOVA: main effect of Satiety: $F_{(1,7)} = 15.45$, $p = 0.006$; no main effect of Frequency: $F_{(3,21)} = 1.46$, $p = 0.26$; no Interaction: $F_{(3,21)} = 0.16$, $p = 0.92$). **J** Stimulation had no effect on latency to lick in eYFP controls (two-way ANOVA: main effect of satiety: $F_{(1,7)} = 56.93$, $p = 0.0001$; no main effect of Frequency: $F_{(3,21)} = 0.19$, $p = 0.90$; no Interaction: $F_{(3,21)} = 0.67$, $p = 0.58$). *$p < 0.05$, **$p < 0.01$, ***$p < 0.001$, ****$p < 0.0001$ Sidak's multiple comparison's post hoc test. $n = 12$ ChR2 and 8 eYFP mice. Data represent mean ± SEM. Source data are provided as a Source Data file.

with AAV-Syn-ChR2-eYFP in the BNST and AAV-DIO-mCherry in the LHA (Fig. 3A). In acute brain slices, whole-cell patch clamp recordings were made from mCherry-expressing neurons within the LHA (Fig. 3B and S4A–C). Blue light pulses elicited time-locked inhibitory post-synaptic currents (IPSCs) that were abolished by application of the GABA$_A$ receptor antagonist, gabazine (Fig. 3C, D). Consistent

with the observation that GABAergic BNST neurons preferentially synapse onto LHA^{Vglut2} neurons[24], 81% (29/36) of synaptically connected LHA^{Vglut2} neurons received GABAergic input (Fig. 3E). The paired-pulse ratio (PPR) of optically evoked IPSCs was unchanged in fasted mice (Fig. 3F). We recorded spontaneous synaptic input onto LHA^{Vglut2} neurons that received GABAergic BNST input and found

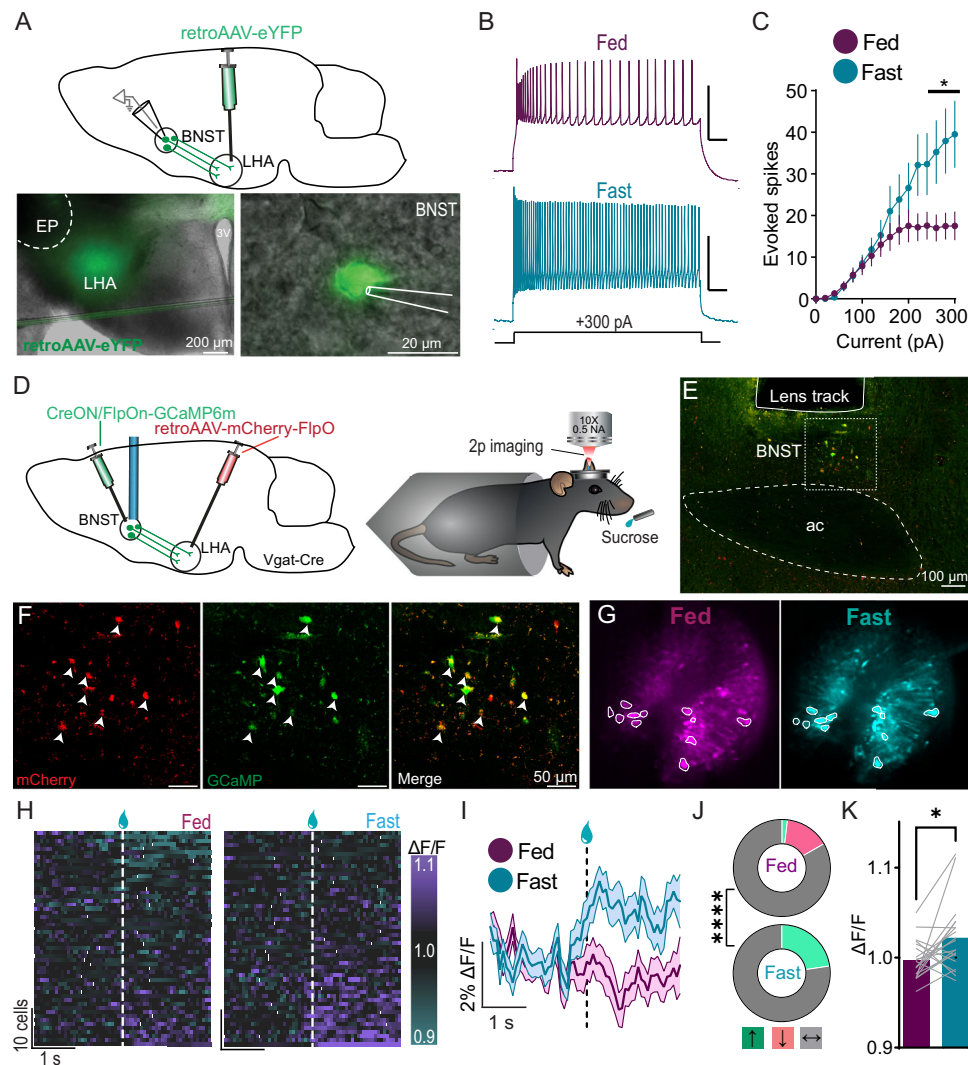**Fig. 2 | Fasting increases excitability and reward responsivity of BNST neurons projecting to LHA. A** Experimental schematic for patching from LHA-projecting BNST neurons. Mice were injected with retroAAV-Syn-eYFP in LHA (bottom left). eYFP-expressing cells were patched in BNST brain slices (bottom right). **B** Example of LHA-projecting BNST neurons recorded from fed (top) and fasted (bottom) mice in response to positive current injection. **C** The number of spikes evoked by large positive current injections was increased in fasted mice (two-way ANOVA: no main effect of Satiety: $F_{(1,31)} = 2.94$, $p = 0.10$; main effect of Current: $F_{(15,465)} = 37.65$, $p < 1.0 \times 10^{-15}$; Interaction: $F_{(15,465)} = 5.69$, $p = 9.07 \times 10^{-11}$). $n = 20/13$ cells from 5/3 mice. *Sidak's post hoc test $p < 0.05$. **D** Experimental schematic. retroAAV-mCherry-FlpO was injected in LHA of Vgat-Cre mice. AAV-CreOn/FlpOn-GCaMP6m was injected in BNST, and a microendoscopic lens was implanted over BNST. BNST^{Vgat}→LHA calcium dynamics were then imaged with 2-photon (2p) microscopy during sucrose consumption. **E** Example lens placement for BNST^{Vgat}→LHA

recordings. **F** High magnification of BNST^{Vgat}→LHA cells (boxed region in **E**) exhibiting co-expression of mCherry and GCaMP (arrows). **G** Example fields of view of BNST^{Vgat}→LHA neurons (mean projection) with cells outlined (13.5 ± 1.1 cells per mouse). **H** BNST^{Vgat}→LHA calcium dynamics aligned to sucrose consumption (dashed line) in ad libitum fed and overnight fasted mice ($n = 53/54$ cells from 4 mice). **I** Average ($\pm$SEM) responses of neurons recorded in fed and fasted mice. Data are smoothed with a rolling average of 3 frames for display purposes. **J** Percentage of cells exhibiting significant excitation (↑), inhibition (↓), or no response (↔) during sucrose consumption. The proportion of cells that were excited was increased by fasting (Fisher's exact test, two-sided, $p = 2.23 \times 10^{-5}$). **K** Average response ($\pm$SEM) of neurons ($n = 20$) tracked across fed and fasted states during the 2 s immediately following the initiation of a consummatory lick bout (two-tailed paired t test, $t(19) = 2.77$, $p = 0.01$). Source data are provided as a Source Data file.

that the rate of IPSCs was increased in fasted mice (Fig. 3G, H). IPSC amplitude was unaffected by fasting (Fig. 3I). The rate and amplitudes of excitatory post-synaptic currents (EPSCs) were also unaffected by fasting (Fig. S4D–F). Consistent with the observation that BNST neurons provide substantial inhibitory input onto LHA^{Vglut2} neurons, we found a strong positive correlation between the optically evoked IPSC amplitude and the amplitude of spontaneous IPSCs (Fig. 3J). These results are consistent with previous recordings of LHA^{Vglut2} neurons across satiety states[26]. Thus, one mechanism underlying increased sensitivity to BNST→LHA stimulation during fasting (Fig. 1) is increased inhibitory strength at the BNST^{Vgat}→LHA^{Vglut2} synapse.

BNST stimulation induces state-dependent LHA^{Vglut2} neuron inhibition in vivo

We next asked whether BNST→LHA stimulation is sufficient to induce inhibition of LHA^{Vglut2} neurons in vivo. To this end, we used a viral strategy in which the red-shifted opsin AAV-Syn-ChrismonR-tdTomato was injected into the BNST and AAV-DIO-GCaMP8m in the LHA of Vglut2-Cre mice. A microendoscopic lens was then implanted above the LHA to allow both optical access to LHA^{Vglut2} neurons as well as optogenetic activation of BNST→LHA fibers (Fig. 4A–C and S5A). Multiphoton calcium imaging of LHA^{Vglut2} cell bodies was conducted using 920-nm pulsed laser light, while optogenetic BNST→LHA axon activation was accomplished by delivering whole-field 620-nm light
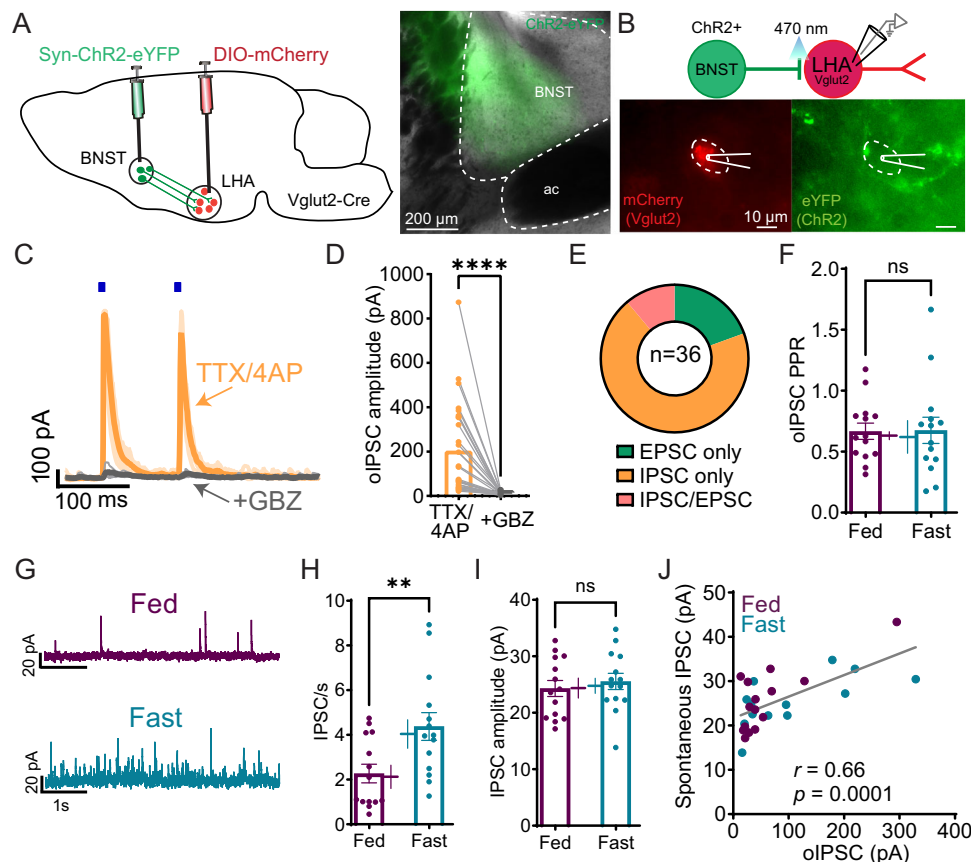
Fig. 3 | Fasting enhances inhibitory tone within the BNST→LHA^{Vglut2} pathway.
A Schematic of viral strategy. AAV-Syn-ChR2-eYFP was injected into BNST and AAV-DIO-mCherry was injected into LHA of Vglut2-Cre mice. Right: example of ChR2 expression in BNST. **B** mCherry-expressing cells adjacent to eYFP+ axons were targeted for whole-cell patch clamp recordings in acute brain slices. **C** Example optically evoked IPSC recorded from an LHA^{Vglut2} neuron in the presence of TTX and 4AP. IPSCs were abolished by applying gabazine (GBZ) to the bath solution. Two 10-ms pulses spaced 100 ms apart were used to evoke IPSCs. Mean value is represented by thick lines and individual sweeps are overlayed. **D** IPSCs are evoked by BNST stimulation in the presence of TTX/4AP and eliminated by the application of gabazine to the bath ($n = 29$ cells from 12 mice; two-tailed paired t test: $t(28) = 5.20$, $p = 1.60 \times 10^{-5}$). **E** Pie chart showing proportion of LHA^{Vglut2} neurons exhibiting optically evoked IPSC, EPSC, or both ($n = 36$ cells from 12 mice). **F** Paired-pulse ratio (PPR) of optically evoked IPSCs was unchanged by fasting (two-tailed t test: $t(26) = 0.06$, $p = 0.96$; $n = 14$ cells from 6 fed mice and $n = 14$ cells from 6 fasted mice). **G** Example traces showing spontaneous IPSCs in fed and fasted mice. Holding current +10 mV. **H** IPSC rate was increased by fasting (two-tailed t test: $t(26) = 2.81$, $p = 0.009$; $n = 14$ cells from 6 fed mice and $n = 14$ cells from 6 fasted mice). **I** IPSC amplitude was unchanged by fasting (two-tailed t test: $t(26) = 0.62$, $p = 0.54$; $n = 14$ cells from 6 fed mice and $n = 14$ cells from 6 fasted mice). **J** Spontaneous IPSC rate and optically evoked amplitude were positively correlated (Pearson $r = 0.66$, $p = 0.0001$). + symbols represent responses averaged (mean ± SEM) for all cells per mouse in (**F**, **H**, **I**). **$p < 0.01$, ****$p < 0.0001$. Source data are provided as a Source Data file.

from an LED through the lens (Fig. 4D)[39]. Pulse trains of 620-nm light were delivered at varying frequencies. To avoid the confound of artifacts from LED stimulation[40], we assessed LHA^{Vglut2} neuron activity immediately following the cessation of stimulation in ad libitum fed and overnight fasted mice. Consistent with the inhibitory composition of the BNST→LHA pathway (Fig. 3E)[24,32,37], we observed inhibition of LHA^{Vglut2} neurons following BNST→LHA stimulation (Fig. 4E–G). The magnitude of LHA^{Vglut2} neuron inhibition increased in accordance with the frequency of stimulation. Interestingly, the magnitude of LHA^{Vglut2} neuron inhibition was greater when mice were fasted compared with when they were ad libitum fed (Fig. 4H and S5B, C). This effect was absent in control mice expressing only a fluorophore in the BNST (Fig. S5D–H). These results agree with our observation that fasting sensitizes mice to BNST→LHA stimulation (Fig. 1) and links our demonstrations of increased inhibitory drive within the BNST→LHA pathway (Figs. 2 and 3) to downstream LHA^{Vglut2} neuron activity.

Overnutrition transiently abolishes state-dependent LHA^{Vglut2} neuron inhibition

We have so far demonstrated that reward seeking evoked by stimulation of BNST axons within LHA is enhanced by fasting and that this is

associated with increased LHA^{Vglut2} neuron inhibition. Because LHA^{Vglut2} neurons are known to become hypofunctional during high-fat diet (HFD) induced obesity[21], we hypothesized that LHA^{Vglut2} neuron inhibition induced by stimulation of BNST inputs would be disrupted following prolonged consumption of HFD. Mice from the previous imaging experiment were given ad libitum access to HFD in their home cages for three weeks. They rapidly increased body weight (Fig. S5I). After three weeks of HFD, BNST→LHA stimulation was again performed while LHA^{Vglut2} neuron calcium activity dynamics were monitored (Fig. 5A, B). Following HFD overnutrition, BNST→LHA stimulation was less effective at inhibiting LHA^{Vglut2} neuron activity. Fasting no longer caused enhanced inhibition of LHA^{Vglut2} neurons following BNST→LHA stimulation (Fig. 5C, D and S5J).

We then tested whether the HFD-induced changes in LHA^{Vglut2} neuron responsivity to BNST→LHA stimulation could be reversed by returning to low-fat chow. Mice were maintained on ad libitum standard chow in their home cages for three weeks, which caused significant weight loss relative to HFD (Fig. S5I). After three weeks on chow, the efficacy of BNST→LHA stimulation in inhibiting LHA^{Vglut2} neurons was again tested (Fig. 5E, F). Strikingly, fasting-potentiated LHA^{Vglut2} neuron inhibition was restored upon return to chow (Fig. 5G,
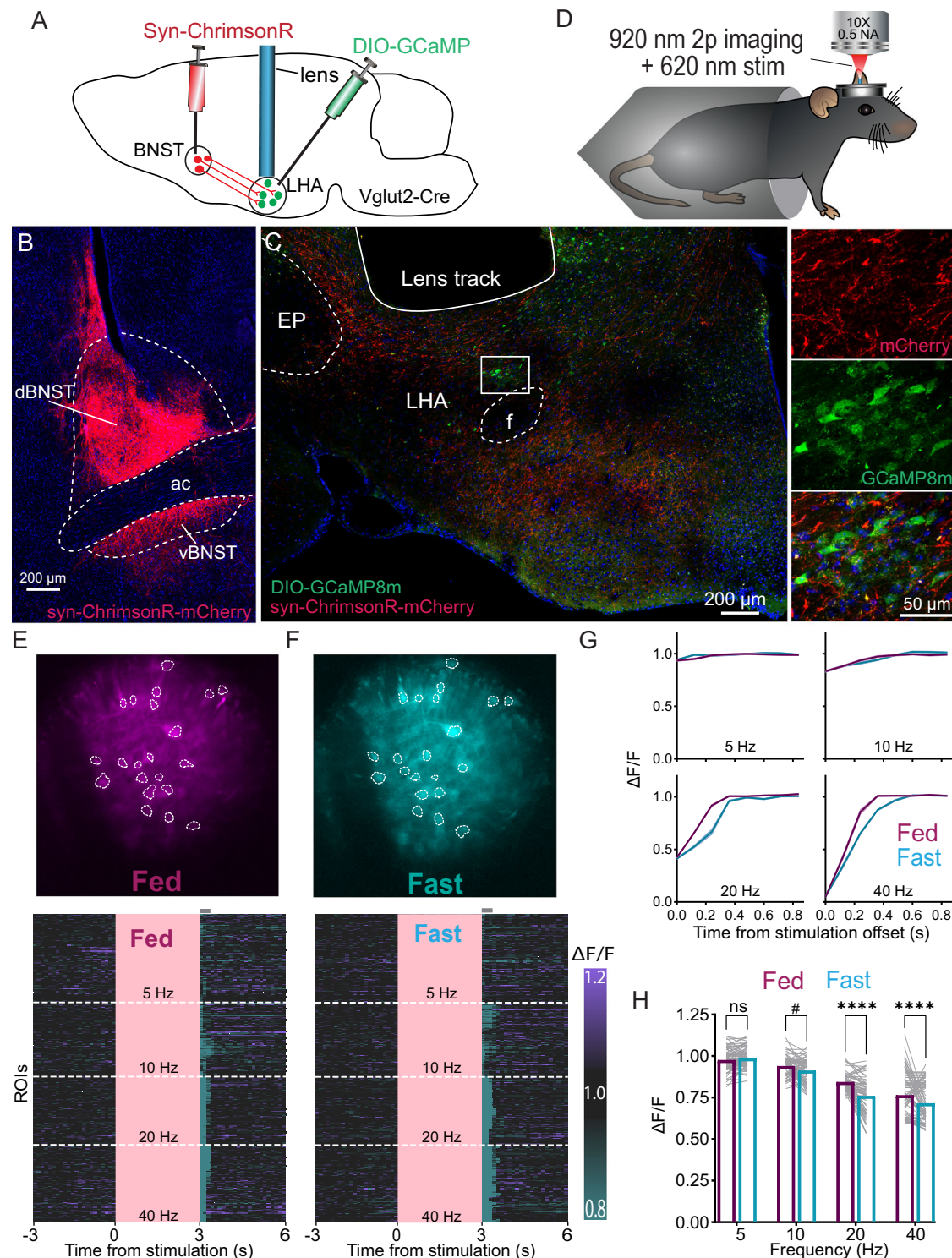
Fig. 4 | Fasting enhances BNST-mediated LHA^{Vglut2} neuron recruitment.
A Schematic of viral strategy. AAV-Syn-ChrimsonR-tdTomato was injected in BNST, and AAV-DIO-GCaMP8m was injected in LHA of Vglut2-Cre mice. A microendoscopic lens was implanted above the LHA. **B** Histological verification of tdTomato expression within the BNST. **C** GCaMP expression was observed in LHA in cells that were closely opposed to tdTomato+ axons under the lens. **D** Experimental schematic for combining two-photon imaging with optogenetic stimulation. **E**, **F** Example imaging plane (standard deviation projection) of LHA^{Vglut2} neurons recorded in fed (**E**) and fasted (**F**) mice with cells outlined (top, 27.5 ± 8.2 cells per mouse). Heat maps show average response of all cells aligned to stimulation onset (bottom). Shaded area represents masked frames corresponding to light artifacts. **G** Average responses ($\pm$SEM) of all recorded neurons aligned to stimulation offset. **H** Average response immediately after the cessation of stimulation (3 frames, 400 ms) for neurons that were recorded in both fed and fasted conditions. Two-way ANOVA: main effect of Satiety: $F_{(1,307)} = 43.38$, $p = 1.96 \times 10^{-10}$, main effect of Frequency: $F_{(3,307)} = 189.40$, $p < 1.0 \times 10^{-15}$, Interaction: $F_{(3,307)} = 12.08$, $p = 1.71 \times 10^{-7}$. Sidak multiple comparison test, ****$p < 0.0001$, #$p = 0.07$. $n = 7$ mice. Source data are provided as a Source Data file.
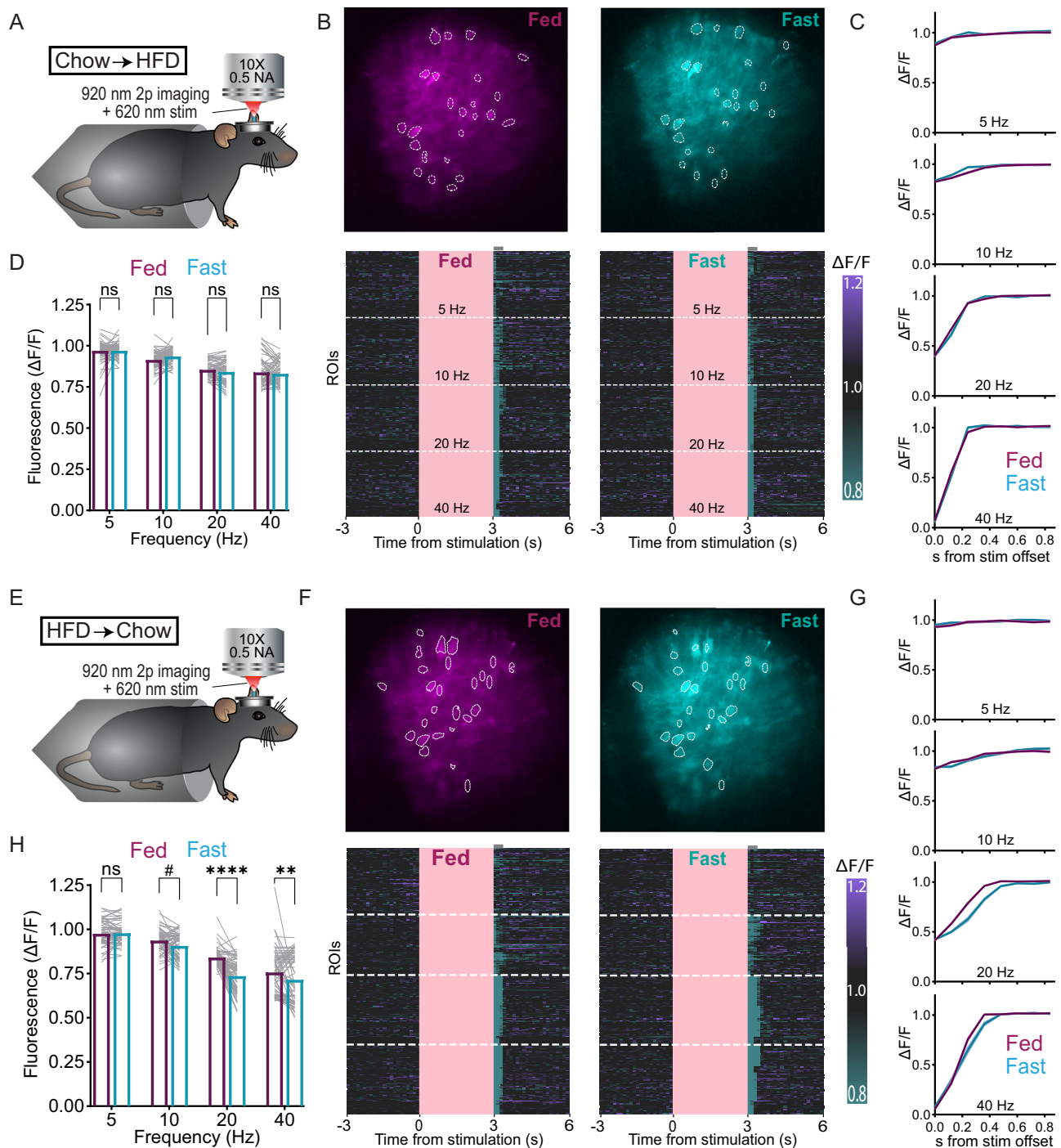
Fig. 5 | Overnutrition transiently impairs BNST-mediated recruitment of LHA^{Vglut2} neurons. A Experimental schematic for HFD overfeeding. Mice were maintained on ad libitum HFD for 3 weeks prior to testing. **B** Example imaging plane (top, standard deviation projection) of LHA^{Vglut2} neurons recorded after over-feeding in fed (left) and overnight fasted (right) mice (25.4 ± 8.2 cells per mouse). Heat maps show average response of all cells from all mice aligned to stimulation onset (bottom). Shaded area represents masked frames corresponding to light artifacts. **C** Average responses ($\pm$SEM) of all recorded neurons aligned to stimulation offset. **D** Average response immediately after the cessation of stimulation (3 frames, 400 ms) for neurons that were recorded in both fed and fasted conditions. Two-way ANOVA: no main effect of Satiety: $F_{(1,256)} = 0.003$, $p = 0.95$, main effect of Frequency: $F_{(3,256)} = 109.6$, $p < 1.0 \times 10^{-15}$, Interaction: $F_{(3,256)} = 2.77$, $p = 0.04$. **E** Experimental schematic for post-HFD imaging. Following HFD, mice were

returned to standard chow for 3 weeks prior to testing. **F** Example imaging plane (top, standard deviation projection) of LHA^{Vglut2} neurons recorded after over-feeding in fed (left) and overnight fasted (right) mice (21.0 ± 5.3 cells per mouse). Heat maps show average response of all cells from all mice aligned to stimulation onset (bottom). Shaded area represents masked frames corresponding to light artifacts. **G** Average responses ($\pm$SEM) of all recorded neurons aligned to stimulation offset. **H** Average response immediately after the cessation of stimulation (3 frames, 400 ms) for neurons that were recorded in both fed and fasted conditions. Two-way ANOVA: main effect of Satiety: $F_{(1,260)} = 53.28$, $p = 3.52 \times 10^{-12}$, main effect of Frequency: $F_{(3,260)} = 143.2$, $p < 1.0 \times 10^{-15}$, Interaction: $F_{(3,260)} = 14.85$, $p = 5.97 \times 10^{-9}$. Sidak multiple comparison test, **$p = 0.002$, ****$p < 0.0001$. $n = 7$ mice. Source data are provided as a Source Data file.
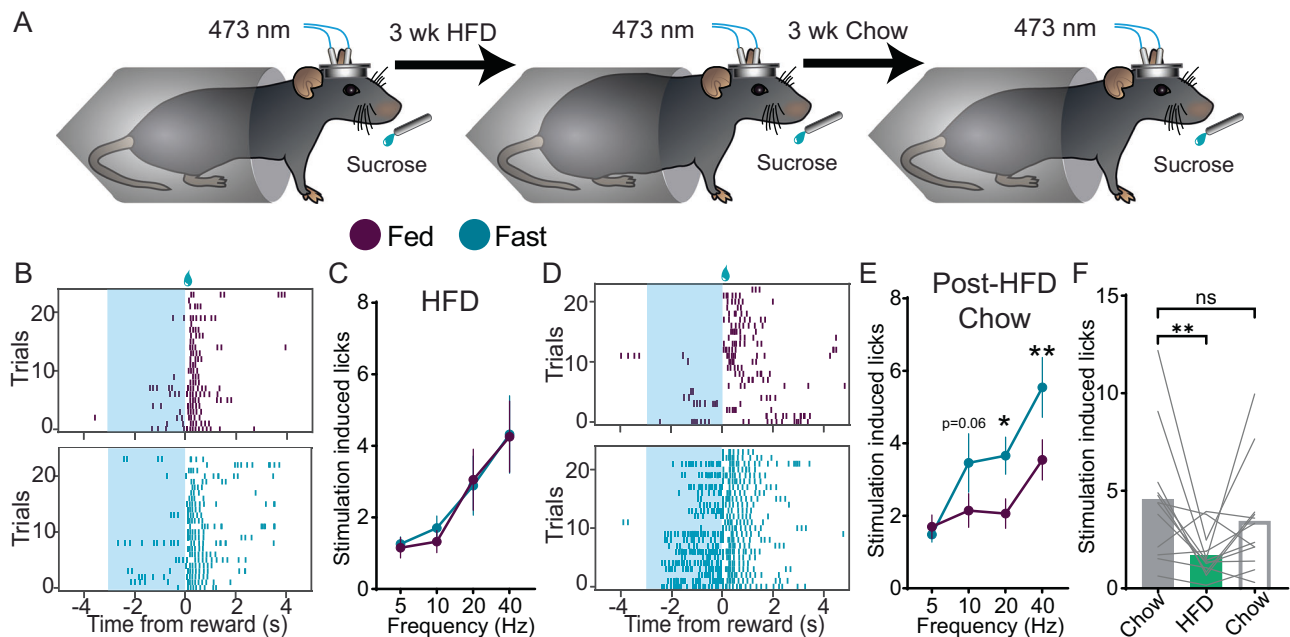
Fig. 6 | State-dependent reward seeking induced by BNST→LHA stimulation is abolished following HFD overnutrition and is partially restored by chow.
A Experimental schematic. Mice with ChR2 in BNST and optic fibers over the LHA were maintained on ad libitum HFD for 3 weeks. Reward seeking in response to BNST→LHA stimulation was then measured. The mice were then returned to chow for 3 weeks, and reward seeking was again measured. **B** Raster plots of licking during fed and fasted conditions during BNST→LHA stimulation following HFD overnutrition. Stimulation was delivered during blue shaded region. **C** Licking during the stimulation period was not increased by fasting following HFD overnutrition (two-way ANOVA: no main effect of Satiety: $F(1,11) = 0.16$, $p = 0.70$; main effect of Frequency: $F(3,33) = 8.24$, $p = 0.0003$; no Interaction: $F(3,33) = 0.31$, $p = 0.82$). Data are mean ± SEM. **D** Raster plots of licking during fed and fasted conditions during BNST→LHA stimulation following return to standard chow. Stimulation was delivered during blue shaded region. **E** Licking during the stimulation period was increased by fasting after mice consumed chow for 3 weeks (two-way ANOVA: main effect of Satiety: $F(1,11) = 15.99$, $p = 0.002$; main effect of Frequency: $F(3,33) = 13.88$, $p = 5.08 \times 10^{-6}$; marginally significant Interaction: $F(3,33) = 2.66$, $p = 0.06$). Data are mean ± SEM. **F** Licks evoked by 10-Hz in fasted HFD overfed mice were reduced compared to chow baseline and rebounded to pre-HFD levels following return to chow. two-tailed one-way ANOVA: $F(2,22) = 6.67$, $p = 0.005$, Dunnet's multiple comparison test: $p = 0.003$ pre-HFD vs HFD; $p = 0.29$ pre-HFD vs post-HFD $n = 12$ mice. $*p < 0.05$, $**p < 0.01$. Source data are provided as a Source Data file.

H and S5K–M). Taken together, these data suggest that HFD overnutrition reduces the ability of the BNST→LHA pathway to recruit LHA^{Vglut2} neurons and that this ability can be rescued by returning to a low-fat environment.

Overnutrition transiently abolishes state-dependent BNST→LHA induced reward seeking
The finding that HFD overnutrition transiently impairs BNST→LHA recruitment of LHA^{Vglut2} neurons led to the hypothesis that reward seeking evoked by BNST→LHA stimulation would also be transiently reduced by overnutrition. To test this possibility, mice with ChR2 or eYFP in the BNST and optic fibers over the LHA were maintained on ad libitum HFD in their home cages for three weeks. Optogenetic testing was then performed as above (Fig. 6A and S6). Consistent with the reduced inhibition observed in LHA^{Vglut2} neurons (Fig. 5A–D), fasting was no longer sufficient to sensitize mice to BNST→LHA stimulation (Fig. 6B, C). While high-frequency stimulation still induced sucrose seeking, low-frequency stimulation was no longer sufficient to potentiate seeking in fasted mice.

We next asked whether changes to inhibitory tone within the BNST→LHA^{Vglut2} pathway underlie the absence of fasting-induced potentiation of reward seeking after HFD. Mice were fed HFD for three weeks. Then, patch clamp recordings were made from LHA^{Vglut2} neurons which receive monosynaptic BNST input (Fig. S7A–D). In mice fed HFD, fasting had no effect on the amplitude or paired-pulse ratio of optically evoked IPSCs (Fig. S7E, F). In contrast to chow fed mice (Fig. 3), HFD fed mice showed no change in inhibitory synaptic inputs during fasting (Fig. S7G–K). Thus, the blunting of both LHA^{Vglut2} activity (Fig. 5) and fasting-induced

enhancement of reward seeking (Fig. 6) are likely mediated by impaired synaptic input during HFD feeding.

To test whether satiety state-dependent reward seeking could be restored by returning to a low-fat chow diet, mice were placed onto ad libitum chow for three weeks. Optogenetic testing was then repeated. Following return to chow, BNST→LHA stimulation again elicited sucrose seeking in a satiety state-dependent manner (Fig. 6D–F). This behavioral plasticity was also apparent in the relationship between stimulation evoked licking and body weight (Fig. S6E–G). When mice were maintained on chow, there was a negative correlation between stimulation evoked licking and body weight that was attenuated by HFD feeding.

LHA^{Vglut2} neurons are necessary for BNST→LHA induced reward seeking
We next tested whether LHA^{Vglut2} neurons are necessary for BNST→LHA stimulation induced reward seeking. Vglut2-Cre mice were injected with AAV-Syn-ChR2-eYFP in the BNST and AAV-DIO-Caspase[41,42] in the LHA (LHA$^{Vglut2-casp}$) to induce apoptotic cell death in LHA^{Vglut2} neurons (Fig. S8A–C). Optic fibers were then implanted above the LHA. Control mice received ChR2 in the BNST and AAV-DIO-eYFP in the LHA (Fig. 7A). Consistent with previous reports[24], LHA$^{Vglut2-casp}$ mice showed no increase in body weight when maintained on chow diet relative to controls (Fig. S8D). However, LHA$^{Vglut2-casp}$ mice exhibited increased chow intake and body weight gain relative to controls during a 6-h refeeding test following an overnight fast (Fig. S8E, F). Three weeks after surgery, mice were habituated to head-fixation, and BNST→LHA induced sucrose seeking was measured. Consummatory behavior was unaffected by LHA^{Vglut2} ablation. However, in both ad libitum fed and
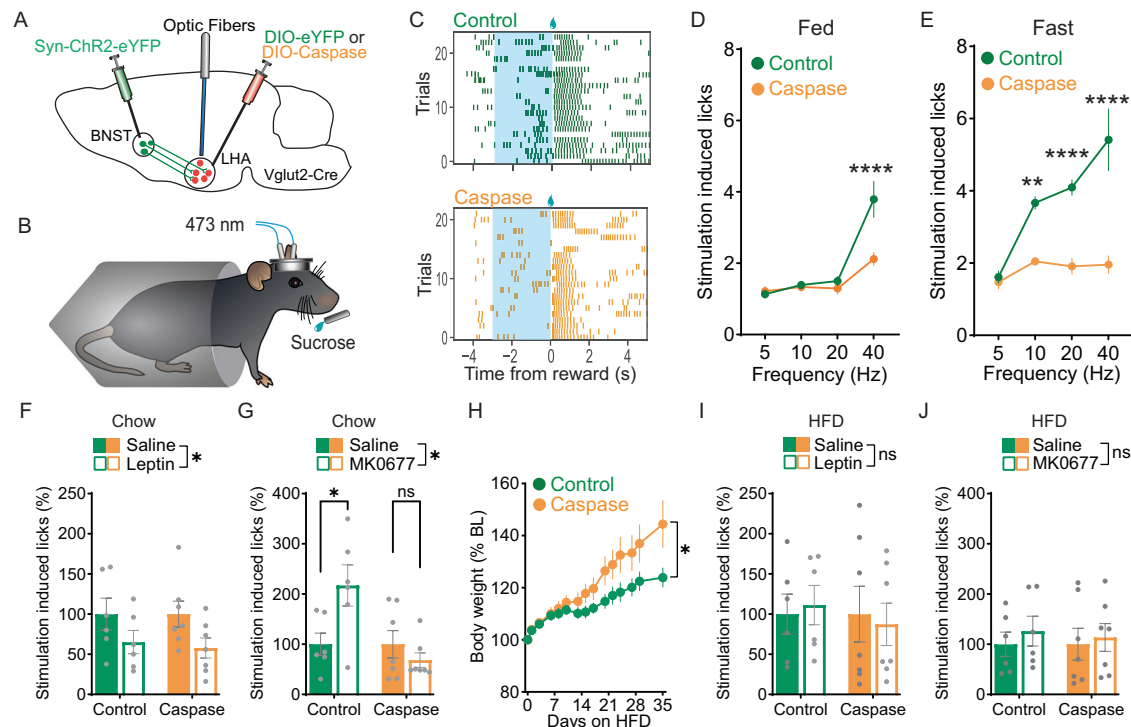
Fig. 7 | Ghrelin signaling on LHA^{Vglut2} neurons is necessary for BNST→LHA stimulation-induced reward seeking. A Schematic of viral strategy. AAV-Syn-ChR2-eYFP was injected in BNST, and either AAV-DIO-taCasp3 or AAV-DIO-eYFP in LHA. Optical fibers were implanted bilaterally above the LHA. **B** Experimental outline. Head-fixed mice consumed randomly delivered drops of sucrose. 473-nm laser stimulation was delivered to the LHA during the 3 s prior to sucrose availability. **C** Example raster plots of licking during fasting for eYFP controls and LHA$^{Vglut2-casp}$ mice. 10hz stimulation is indicated by the blue shaded region. **D** Appreciable stimulation induced licking was observed only at high-frequency stimulation and was reduced in ad libitum fed LHA$^{Vglut2-casp}$ mice (two-way ANOVA: main effect of Group: $F(1,11) = 7.14$, $p = 0.02$; main effect of Frequency: $F(3,33) = 35.41$, $p = 1.99 \times 10^{-10}$; Interaction: $F(3,33) = 8.54$, $p = 0.0002$). **E** Stimulation induced licking was significantly reduced in fasted LHA$^{Vglut2-casp}$ mice (two-way ANOVA: main effect of Group: $F(1,11) = 44.45$, $p = 3.53 \times 10^{-5}$; main effect of Frequency: $F(3,33) = 16.87$, $p = 8.10 \times 10^{-7}$; Interaction: $F(3,33) = 9.94$, $p = 8.14 \times 10^{-5}$). $^{**}p < 0.01$, $^{****}p < 0.0001$ Sidak's multiple comparisons post hoc test. **F** Leptin suppresses BNST→LHA stimulation induced licking even in LHA$^{Vglut2-casp}$

mice (two-way ANOVA: no main effect of Group: $F(1,11) = 0.06$, $p = 0.81$; main effect of Leptin: $F(1,11) = 5.42$, $p = 0.04$; no Interaction: $F(1,11) = 0.05$, $p = 0.83$). **G** The GHSR agonist, MK0677, fails to potentiate BNST→LHA stimulation induced licking in LHA$^{Vglut2-casp}$ mice (two-way ANOVA: main effect of Group: $F(1,11) = 7.17$, $p = 0.02$; no main effect of MK0677: $F(1,11) = 2.62$, $p = 0.13$; Interaction: $F(1,11) = 7.91$, $p = 0.02$). *Sidak's multiple comparisons post hoc test, $p < 0.05$. **H** LHA$^{Vglut2-casp}$ mice are prone to HFD-induced obesity. Body weight during 5 weeks of HFD access (two-way ANOVA: no main effect of Group: $F(1,11) = 2.24$, $p = 0.16$; main effect of Time: $F(14,154) = 36.67$, $p < 1.0 \times 10^{-15}$; Interaction: $F(14,154) = 3.96$, $p = 8.49 \times 10^{-6}$). **I** Following prolonged HFD consumption, leptin no longer suppresses BNST→LHA stimulation induced licking in either control or caspase mice (two-way ANOVA: no main effects of Group and no Interaction, $p > 0.5$). **J** Following prolonged HFD consumption, MK0677 no longer potentiates BNST→LHA stimulation induced licking in control mice (two-way ANOVA: no main effects of Group and no Interaction, $p > 0.5$). n = 6 control and 7 caspase mice. Data are mean ± SEM. Source data are provided as a Source Data file.

overnight fasted conditions, LHA$^{Vglut2-casp}$ mice showed significantly reduced optically evoked sucrose seeking relative to controls (Fig. 7B–E). LHA$^{Vglut2-casp}$ mice still responded to high-frequency stimulation, albeit to a lesser extent than controls. This difference was not observed on trials in which laser stimulation was not delivered (Fig. S8G). Consistent with our previous observation that BNST→LHA stimulation fails to drive aberrant consummatory behavior (Fig. S2), LHA$^{Vglut2-casp}$ mice showed similar levels of licking when BNST→LHA stimulation was delivered concurrently with sucrose availability (Fig. S8H-I). Thus, LHA^{Vglut2} neurons are required for BNST→LHA induced reward seeking but are dispensable for consummatory behavior. This agrees with our previous work showing only a weak relationship between LHA^{Vglut2} neuron activity and motor aspects of consummatory licking[21,26].

Feeding hormones bidirectionally regulate BNST→LHA^{Vglut2} mediated reward seeking

Finally, we tested whether hormonal signals regulating hunger and satiety underlie the increased sensitivity to BNST→LHA stimulation during fasting. Leptin is an anorexigenic hormone that is produced by adipose tissue and is associated with appetite suppression. Ghrelin is

an orexigenic hormone that is produced in the gut and promotes hunger. Both leptin and ghrelin are known to act within the LHA, including on LHA^{Vglut2} neurons, to influence feeding behavior[26,43,44]. Circulating levels of leptin and ghrelin fluctuate according to energy state to influence feeding[45–47]. We tested whether leptin and ghrelin administration influences BNST→LHA stimulation induced sucrose seeking in control and LHA$^{Vglut2-casp}$ mice. Systemic leptin administration in fasted mice reduced BNST→LHA evoked sucrose seeking in both control and LHA$^{Vglut2-casp}$ mice (Fig. 7F). In contrast, agonizing the ghrelin receptor (growth hormone secretagogue receptor, GHSR) with the selective agonist MK0677[48] in ad libitum fed mice only potentiated BNST→LHA induced sucrose seeking in control but not LHA$^{Vglut2-casp}$ mice (Fig. 7G). Following prolonged consumption of HFD, which exacerbated weight gain in LHA$^{Vglut2-casp}$ mice (Fig. 7H)[25], both control and LHA$^{Vglut2-casp}$ mice showed insensitivity to the effects of leptin and MK0677 (Fig. 7I, J). These results demonstrate that satiety-state-dependent modulation of BNST→LHA induced reward seeking can be recapitulated by hunger and satiety hormones. While suppression of BNST→LHA induced sucrose seeking by leptin is still observed in LHA$^{Vglut2-casp}$ mice, they are unresponsive to MK0677. This suggests GHSR signaling on LHA^{Vglut2} neurons underlies the increased sensitivity

to BNST→LHA stimulation during fasting. Furthermore, the finding that control mice cease responding to GHSR agonism after HFD overnutrition suggests that insensitivity to ghrelin causes the insensitivity to BNST→LHA stimulation induced reward seeking during fasting following prolonged HFD consumption.

Together, these results indicate that the BNST→LHA pathway is critical for guiding reward seeking behavior according to current energy demands. During fasting when available energy stores are depleted, ghrelin levels are high and leptin levels are low. The same stimulation induces more robust behavioral responses compared to when mice are ad libitum fed and ghrelin levels are low and leptin levels are high. This effect depends on the integrity of LHA^{Vglut2} neurons and likely involves changes at the BNST^{Vgat}→LHA^{Vglut2} synapse. Following overnutrition in which an energy surplus exists, BNST→LHA^{Vglut2} neuron recruitment is diminished, leading to impaired ability to influence reward seeking. This is likely mediated by insensitivity to peripherally derived hunger and satiety signals, including leptin and ghrelin.

Discussion

These data identify energy state-dependent control of reward seeking through the BNST→LHA^{Vglut2} pathway. Previous studies have ascertained a key function of GABAergic BNST inputs to the LHA in promoting food consumption and have suggested that GABAergic BNST neurons synapse primarily onto glutamatergic LHA neurons[24,32]. Our findings demonstrate that the ability of BNST→LHA pathway activation to promote appetitive behavior requires LHA^{Vglut2} neurons and depends upon the current energy state. Optogenetic activation of this pathway leads to frequency-dependent changes in both reward seeking (Fig. 1) and downstream LHA^{Vglut2} activity (Fig. 4). These effects are potentiated by fasting. In support of this, electrophysiological recordings found stronger inhibitory tone within the BNST→LHA^{Vglut2} pathway following an overnight fast (Fig. 3) and increased excitability and reward responsivity in BNST→LHA neurons (Fig. 2). Additionally, overnutrition transiently blunts both state-dependent induction of reward seeking through BNST→LHA pathway activation as well as LHA^{Vglut2} neuron inhibition (Figs. 4–6). The effects of overnutrition on BNST→LHA^{Vglut2} activity and function are recoverable by returning to a low-calorie diet. The ability of BNST→LHA pathway activation to elicit state-dependent reward seeking was abolished when LHA^{Vglut2} neurons were ablated and could be recapitulated by administration of hunger and satiety hormones (Fig. 7). Taken together, our findings suggest that inhibitory BNST neurons regulate food reward seeking in response to changing energy demands via projections to LHA^{Vglut2} neurons. Fasting or GHSR agonism sensitizes neurons within this pathway to promote feeding when energy stores are low. Overnutrition disrupts these processes and desensitizes reward seeking elicited by BNST→LHA stimulation, which can be rescued by returning to a low-calorie diet.

Mechanisms of state-dependent functional changes

Numerous studies have highlighted functionally heterogenous LHA neuron populations that promote various motivated behaviors including reward seeking and food consumption[4,8,10,18,20,21,24,26,49]. Among these, LHA^{Vglut2} neurons have been hypothesized to act as a "brake" on feeding behavior. Acute LHA^{Vglut2} neuron activation suppresses reward seeking and food intake, and subsets of LHA^{Vglut2} neurons show reduced activation following an overnight fast[21,24,25,28]. Our findings agree with these studies and extend our understanding of how LHA^{Vglut2} neurons orchestrate behavior according to changing energy demands. LHA^{Vglut2} neurons are downstream targets of GABAergic BNST neurons (Fig. 3)[24]. Consistent with this, activation of the BNST→LHA pathway promotes food reward seeking by inhibiting LHA^{Vglut2} neurons. Optogenetic BNST→LHA stimulation inhibits LHA^{Vglut2} neurons in vivo (Fig. 4), and LHA^{Vglut2} neuron ablation

eliminates stimulation-induced sucrose seeking (Fig. 7). Previous work has demonstrated that subsets of LHA^{Vglut2} neurons exhibit reduced responding to food rewards during fasting[21]. Our observation that LHA^{Vglut2} neurons also receive enhanced inhibitory synaptic input during fasting and that BNST^{Vgat}→LHA neurons are more responsive to sucrose rewards is consistent with these findings.

Previous studies have also shown that HFD overfeeding reduces the ability of LHA^{Vglut2} neurons to respond to food consumption with excitatory bursts of activity[21,24]. We found that following HFD overfeeding, BNST→LHA stimulation-induced reward seeking becomes insensitive to changes in hunger state. When mice are fasted after overconsuming HFD, they no longer show increased sucrose seeking relative to when they are ad libitum fed (Fig. 6). This is associated with reduced inhibition of LHA^{Vglut2} neurons (Fig. 5). HFD overfeeding also eliminates the fasting-induced enhancement of inhibitory synaptic input to LHA^{Vglut2} neurons (Fig. S7). Together, these results suggest that HFD exerts changes both within the BNST→LHA^{Vglut2} pathway as well as on the wider LHA^{Vglut2} neuron population. Here, we show that the BNST→LHA^{Vglut2} pathway is critical for regulating behavioral responses to changes in energy needs during fasting, which is disrupted by three weeks of HFD exposure. However, with longer HFD exposure, the LHA^{Vglut2} population shows persistent hyporesponsivity during food consumption[21]. Given the observation that LHA^{Vglut2} neurons are hypoactive during HFD feeding, it stands to reason that stimulation of BNST GABAergic inputs fails to further inhibit LHA^{Vglut2} neurons during fasting (ie, a 'floor' effect). Thus, stimulation of the BNST→LHA pathway fails to potentiate sucrose seeking during fasting after HFD exposure (Fig. 5 & 6). Because previous work did not examine the relationship between fed and fasted states in the context of HFD overfeeding, future studies will be needed to elucidate the mechanisms driving the suppression of LHA^{Vglut2} neurons during chronic HFD overfeeding. We speculate that prolonged HFD consumption causes dysfunction within the LHA^{Vglut2} neuron population through mechanisms that may be independent of BNST synaptic input.

Role of feeding hormones in BNST→LHA^{Vglut2} mediated reward seeking

Our data indicate that hormonal signals play a critical role in mediating the ability of the BNST→LHA stimulation to induce food reward seeking (Fig. 7). BNST→LHA stimulation evokes robust sucrose seeking when mice are fasted overnight. This energy state-dependent sensitization can be recapitulated by administering a GHSR agonist to ad libitum fed mice. Similarly, mice are relatively insensitive to BNST→LHA stimulation when they are ad libitum fed. This insensitivity can be replicated by administering the anorexigenic hormone leptin to fasted mice. These data confirm that the behavioral sensitization observed during fasting is not stress-induced. Moreover, ablating LHA^{Vglut2} neurons prevents GHSR-agonist induced sensitization without affecting the ability of leptin to suppress BNST→LHA stimulation induced feeding. This suggests that GHSR activation is likely a critical mechanism contributing to the enhanced excitability within the BNST→LHA^{Vglut2} pathway observed during fasting. Leptin and ghrelin are widely known to influence behavior via the lateral hypothalamus[28,43,44,50,51]. Indeed, both leptin receptor and GHSR are expressed within the LHA, including on a subset of LHA^{Vglut2} neurons[26]. Future studies will be needed to determine if these hormones exert their effects by acting directly on LHA^{Vglut2} neurons or through circuit-level interactions. Given the widespread expression of leptin receptor and GHSR within the brain, it is likely that these hormones enhances food motivation via multiple routes[47,48,52], including in the BNST[53]. The observed insensitivity to BNST→LHA stimulation after HFD overfeeding mirrors previous findings in studies of appetite-promoting agouti-related peptide (AgRP) neurons. AgRP neurons, which are typically activated by ghrelin to drive feeding behavior, become less responsive to ghrelin following prolonged HFD consumption[54,55]. This adaptation is thought to

contribute to the dysregulation of energy balance in obesity, as ghrelin's ability to stimulate hunger becomes impaired, which is in line with our observations. Regardless of direct action, our data demonstrate that LHA[Vglut2] neurons are required for ghrelin−but not leptin−to mediate the behavioral response to BNST→LHA stimulation.

Sensitivity to BNST→LHA stimulation is bidirectionally modified by natural hunger states as well as feeding hormones. We therefore speculate that the observed behavioral and neuronal changes likely occur on timescales matching natural hormonal fluctuations. Leptin and ghrelin fluctuate around meal time to influence food intake[46,56]. Here, we demonstrate that this hormonal feedback is necessary and sufficient to alter sensitivity to BNST→LHA stimulation induced reward seeking. We hypothesize that under natural hunger states, the rise in ghrelin preceding meal initiation is accompanied by an increase in excitability of BNST→LHA neurons. After satiation, the fall in ghrelin levels and slow rise in leptin levels is expected to reduce the excitability of these neurons. Exactly how long it takes after satiation for insensitivity to BNST→LHA stimulation to occur remains to be determined.

HFD-induced impairment of BNST→LHA[Vglut2] function

Whereas fasting causes mice to become more sensitive to BNST→LHA stimulation, HFD overnutrition blunts the behavioral response (Figs. 5−7)[24]. HFD overfeeding reduces both motivation for food and preference for palatable foods in rodents[57−61]. Similarly, people with obesity or those who consume obesogenic foods have impaired sensitivity to rewarding aspects of food[62−65]. Thus, our results are in agreement with these observations. While fasting increases motivation, HFD overfeeding decreases motivation. This is recapitulated in the changes in responsivity to BNST→LHA stimulation and is accompanied by altered physiology in the BNST→LHA[Vglut2] pathway.

LHA[Vglut2] neuron activation suppresses feeding[18,21,24,25]. Similarly, stimulation of GABAergic inputs is expected to inhibit LHA[Vglut2] neurons and promote feeding. Here, we show that enhanced LHA[Vglut2] neuron inhibition during fasting is caused by increased GABAergic input originating at least in part within the BNST. However, other inhibitory inputs, including arcuate AgRP and LHA GABAergic neurons, influence LHA[Vglut2] function[27,66] and are sensitive to energy state[67,68]. This increased inhibitory tone during fasting allows LHA[Vglut2] neurons to exhibit more sustained inhibition during BNST→LHA stimulation, thereby facilitating reward seeking. In support of their proposed role as a 'brake' on feeding, HFD consumption decreases LHA[Vglut2] neuron excitability and their responses to sucrose rewards[21]. Interestingly, the present results demonstrate that energy state-dependence of BNST-mediated inhibition of LHA[Vglut2] neurons is eliminated by HFD consumption (Fig. 5). This is accompanied by impaired sensitivity to leptin and MK0677 and reduced ability of BNST→LHA stimulation to induce reward seeking according to current energy state.

Importantly, once mice have consumed HFD, we observed recovery of function and physiology when they are returned to a low-fat diet (Figs. 5 and 6). Weeks after returning to a chow diet, we see that both state-dependent BNST→LHA induced reward seeking and LHA[Vglut2] neuron inhibition return. The behavioral phenotype observed in response to optogenetic BNST→LHA stimulation shows a remarkable parallel to the LHA[Vglut2] neuronal activity. These results suggest that the effects of HFD on neurocircuit function may be reversible, which is consistent with studies showing partial restoration of brain function following weight loss[69−71]. The degree to which brain function can be rescued is likely determined by the duration of HFD consumption as well as recovery time.

Functional heterogeneity within LHA[Vglut2] neurons

Previous recording and single cell sequencing studies have highlighted the considerable functional and molecular heterogeneity within the LHA[Vglut2] neuron population[18,19,21,26]. Consistent with this, we observe a range of LHA[Vglut2] neuronal responses induced by BNST stimulation (Figs. 4 and 5). At low frequencies, LHA[Vglut2] neuronal responses are quite varied, with cells exhibiting inhibition, mild excitation, or no response to stimulation. With increasing stimulation frequency, LHA[Vglut2] neurons are more uniformly inhibited. This suggests that local microcircuits may be involved. Such microcircuitry remains to be clarified. However, the increased degree of LHA[Vglut2] neuron inhibition observed after high frequency stimulation is consistent with our behavioral results.

It has been proposed that LHA[Vglut2] neurons projecting to discrete downstream targets exhibit unique molecular signatures and contribute to distinct aspects of behavior[4,10,18,26]. It remains to be determined whether molecularly or anatomically defined LHA[Vglut2] neuron populations may correspond to cells that are recruited by BNST→LHA stimulation at various frequencies. An appealing possibility is that LHA[Vglut2] neurons that are highly sensitive to BNST stimulation send their axons to the lateral habenula (LHb). The LHb is a major destination for LHA[Vglut2] axon terminals. Activation of LHA[Vglut2]→LHb neurons reliably suppresses feeding[18,25]. Their responses to sucrose consumption are modified by satiety state as well as leptin and ghrelin[26], and LHb-projecting LHA[Vglut2] neurons receive synaptic input from the BNST[18]. Thus, the LHb is likely to be a primary downstream effector of the LHA[Vglut2] neurons contributing to the present results. However, LHA[Vglut2] neurons also project to other brain regions, including the medial thalamus[25] and ventral tegmental area[26,72]. Future studies are needed to elucidate the downstream circuit architecture underlying BNST→LHA[Vglut2] stimulation induced reward seeking as well as their contributions to other reward-related behaviors.

BNST involvement in promoting reward seeking

In agreement with previous findings, we found that high frequency optogenetic stimulation of the BNST→LHA pathway promotes food seeking[24]. Interestingly, most BNST→LHA neurons exhibited low basal firing rates in brain slices but are capable of sustained firing at frequencies greater than 20 Hz (Fig. 2B, C, S3B, C). This suggests that BNST→LHA neurons are not highly active under resting conditions but can exhibit high and sustained firing in response to stimulation. Our in vivo recording data suggest greater levels of synchronous activity during appetitive and consummatory behavior (Fig. 2I). This is likely driven by synaptic input to BNST neurons, but the source of this input remains to be elucidated.

BNST[Vgat]→LHA neurons begin to increase activity prior to sucrose consumption. Especially when mice are fasted, these neurons begin to respond well before consumption occurs. This suggests that these neurons are active both during the appetitive and consummatory phases of feeding. Consistent with this possibility, stimulation of BNST→LHA neurons is sufficient to promote food seeking and consumption[24]. We hypothesize that BNST→LHA neurons naturally contribute to the initiation of appetitive licking. Strong activation of this pathway through either high-frequency stimulation or a combination of low-frequency stimulation and fasting can trigger appetitive licking. Interestingly, we find that ~22% of BNST[Vgat]→LHA neurons are activated prior to and during sucrose consumption (Fig. 2H−J). Additionally, many BNST[Vgat]→LHA neurons have responses that are tuned to different tastants and motivational states (Fig. S3J, K). This suggests that the BNST[Vgat]→LHA neuron population may guide seeking of distinct reward types via discrete activity patterns. One possibility that remains untested is whether anatomically or molecularly defined BNST[Vgat]→LHA neurons contribute to unique aspects of behavior. Recently, molecularly distinct GABAergic BNST neuron populations, including some projecting to the LHA, have been defined[32,73]. Future studies will be needed to parse how distinct BNST GABAergic subpopulations encode unique types of rewards and whether they synapse onto LHA[Vglut2] neurons.

Limitations of the current study

One important limitation of the current study is the use of head-fixed behavioral assays. This method was chosen because it permits reliable manipulation of neural activity during specific aspects of reward seeking behavior. It also allows us to link behavioral phenotypes observed during optogenetic stimulation with two-photon calcium imaging data. However, head-fixed behavior has limitations. It can be stressful for the animals and is less ethologically relevant than tasks in which animals are allowed to move freely. It has previously been demonstrated that activation of the GABAergic BNST→LHA pathway induces both food seeking and consumption in freely moving mice[24]. Interestingly, we observed only an increase in food seeking but not consummatory behavior. Whether this would be true if food remained available during prolonged stimulation in head-fixed mice remains to be determined. These results highlight the role of behavioral context on the function of this pathway. Future studies will be required to fully elucidate how BNST[Vgat]→LHA[Vglut2] circuitry contributes to distinct aspects of behavior across different contexts.

In conclusion, we have shown that the inhibitory BNST→LHA pathway is a critical mediator of reward seeking behavior. The degree of reward seeking is directly related to the ability of BNST neurons to inhibit LHA[Vglut2] neurons according to energy needs. The ability of this pathway to elicit reward seeking requires LHA[Vglut2] neurons and is regulated by hunger and satiety hormones, processes that are disrupted during HFD-induced overnutrition. Together, these results indicate one way in which brain circuits orchestrate reward seeking behavior to meet current energy demands, which may be dysfunctional in obesity. Our results suggest that the function of the BNST→LHA[Vglut2] pathway can be rescued after overnutrition by returning to a low-fat diet and provide insights for future targeted interventions.

Methods

Mice

Male and female mice on C57BL/6 background were obtained from Jackson Laboratory. For optogenetic experiments without caspase and BNST patching experiments, wild-type C57BL/6 J mice were used. Vgat-ires-Cre mice (Jackson Laboratory strain #028862)[74] were used for BNST imaging. For all other experiments, Vglut2-ires-Cre mice (Jackson Laboratory strain #028863)[74] were used. Detailed breakdowns of age and sex for each experiment can be found in the corresponding methods description. Mice were maintained on a 12-hour light-dark cycle with access to food and water ad libitum in their home cages. Room temperature was 21-23 °C and humidity was 30-70%. Unless specified for fasting experiments, mice had continuous access to food and water in their home cages. Except for during high-fat diet testing, mice were fed standard chow (Purina 5058 mouse chow, 21% fat calories). All procedures were conducted following the National Institutes of Health Guide for the Care and Use of Laboratory Animals and were approved by the Rutgers University Institutional Animal Care and Use Committee.

Surgery

Mice were anesthetized with isoflurane (maintained at <1.5%) and positioned in a stereotaxic frame (Kopf Instruments). Ophthalmic ointment was applied to the eyes, and bupivacaine (2 mg/kg) was injected subcutaneously at the incision site. Post-surgery, 5 mg/kg carprofen was administered intraperitoneally. All viruses were delivered through stainless steel injectors at a rate of 100 nL/min. Injectors were kept in place for at least 10 min after each infusion.

For optogenetic experiments, wild-type c57BL/6J mice (ChR2: $n = 5$ F/7 M, eYFP: $n = 4$ F/4 M) were used. Burr holes were drilled bilaterally above the BNST. An adeno-associated virus carrying ChR2 (AAV5-hSyn-ChR2-eYFP, 400 nL; UNC Viral Vector Core, titer: 5.3×10^{12}) or eYFP (AAV5-hSyn-eYFP; UNC Viral Vector Core, titer: 5.6×10^{12} was

injected into the BNST at the following coordinates relative to Bregma: AP + 0.15, ML + 0.9, DV −3.85 (from brain surface) using a custom steel injection cannula. 200 μm core optical fibers (RWD Life Sciences) were bilaterally implanted ~150 μm above the LHA at a 6° from vertical and secured in place with dental cement. A stainless-steel head fixation ring was also cemented atop each mouse's head.

For caspase experiments, Vglut2-Cre mice (Caspase: $n = 5$ M/2F, control: $n = 5$M/1F) were injected bilaterally with either AAV5-FLEX-taCasp3-TEVP (UNC Viral Vector core, titer: 4.2×10^{12}) or AAV5-Ef1a-DIO-eYFP (UNC Viral Vector Core, titer: 4.1×10^{12}) 400 nl in LHA and AAV5-hSyn-ChR2-eYFP, 300 nL (UNC Viral Vector Core) in BNST. Optic fibers (RWD Life Sciences) were bilaterally implanted ~150 μm above the LHA at a 6° from vertical and secured in place with dental cement. A stainless-steel head fixation ring was also cemented atop each mouse's head. Mice recovered 4 weeks before optogenetic testing began.

For two-photon imaging experiments, Vglut2-Cre mice ($n = 7$ M) were injected unilaterally with 300 nL AAV5-Syn-ChrimsonR-tdTomato (UNC viral vector core, titer: 4.6×10^{12}) in BNST and 400 nL of AAV5-syn-FLEX-jGCaMP8m-WPRE (Addgene #162378, titer: 2.4×10^{13}) in LHA at −1.35 AP, +0.95 ML, −5.15 DV from the brain surface. Next, a 0.6 mm diameter × 7.3 mm length GRIN lens (Inscopix) was slowly lowered into place above the ~200 μm above the injection site and affixed with dental cement. Finally, a head fixation ring was placed on the skull with the lens in the center, and everything was secured in place with dental cement and skull screws. Surgeries for fluorophore control imaging were performed as described above except AAV5-CAG-tdTomato (UNC viral vector core, titer: 3.2×10^{12}) was injected unilaterally to the BNST and AAV5-syn-FLEX-jGCaMP8m-WPRE was injected in LHA in Vglut2 mice ($n = 4$ M). A lens was then implanted above the LHA. Surgeries for BNST imaging were performed as described above except retroAAV-EF1α-mCherry-Ires-FlpO[75] was injected in LHA and AAV8-CreON/FlpOn-GCaMP6m[38] was injected in BNST in Vgat-Cre mice ($n = 4$ M). A lens was then implanted above the BNST.

For LHA[Vglut2] patching experiments, Vglut2-Cre mice (Chow Fed: $n = 2$M/4F, Chow Fast: $n = 2$M/4F, HFD Fed: $n = 2$M/3F, HFD Fast: $n = 5$M/2F) were injected bilaterally with AAV5-hsyn-ChR2-eYFP (300-400 nL) in BNST and AAV5-DIO-mCherry (UNC Vector Core, titer: 5.1×10^{12}, 500 nL) in LHA. For BNST patching experiments, wild-type mice (Fed: $n = 3$M/1F, Fast: $n = 2$M/3F) were injected with retroAAV-Syn-eYFP in LHA. Mice recovered 3–4 weeks before testing began.

Head fixed behavior with optogenetics

Head fixed optogenetic stimulation experiments were performed as previously described[21,26]. Following recovery from surgery and prior to optogenetic stimulation experiments, mice were habituated to head fixation for 3 days, during which unpredictable drops of sucrose (10% sucrose in water; 2.0–2.5 μL, inter-trial interval 25–30 s) were delivered intermittently for 30 min through a gravity-driven, solenoid-controlled lick tube. On optogenetic test days, mice were head fixed and connected to a 473-nm DPSS laser. Test sessions consisted of 50 trials in which 2 μL of 10% sucrose solution was randomly delivered via a tube placed directly in front of the mouse's mouth. Once the mice displayed sufficient licking, they were subsequently put in a 50-trial task, of which a randomized half of the trials contained optogenetic stimulations (5, 10, 20 and 40 Hz, 5 ms pulse width, 10 mW) of a given frequency for 3 s prior to reward delivery. The stimulation frequency was constant during a session but pseudo-randomized between sessions. Licks were recorded during the entire session. For experiments in which stimulation was delivered during reward availability, stimulation was 20 Hz, 5 ms pulse width, 10 mW for 3 s starting at the time of reward delivery. Mice were kept food restricted at 85–90% baseline body weight during initial conditioning. Once the mice displayed sufficient licking behavior, they were either kept ad libitum fed (Purina 5058 mouse chow, 21% fat calories) or fasted overnight for each of the optogenetic stimulation sessions. After all stimulations were performed for all mice in

fed and fasted states, mice were put onto HFD (60% animal fat calories; Bio-Serv #F3282) for 3 weeks. Mice were 4-6 months and weighed 21–33 g at the start of HFD exposure. Optogenetic experiments were resumed, with mice kept either ad lib fed or fasted for 24 h through each of the stimulations. After all frequencies were performed for all mice in fed and fasted, mice were returned to ad lib chow diet for 3 weeks. For experiments in which mice were provided sucrose and quinine, mice were given access to 2 solutions, 10% sucrose in water, and 1.5 mM quinine, in a 2:1 ratio across the 75 trials. Before the experiments, mice were kept food or water deprived overnight. Once the mice displayed sufficient licking in response to the sucrose rewards, the behavior sessions were conducted with optogenetic stimulations delivered for 3 s starting at reward delivery for a randomized 50% of the trials.

Overnight fasting-induced refeeding
Mice were singly housed, and chow was removed from home cages at ~5 p.m. and mice were given a clean cage bottom. Mice had *ad libitum* access to water during food deprivation. The following morning between 8 and 9 a.m., fasted mice were given chow pellets. Food intake and body weight were measured at 2, 4 and 6 h. Following the experiment, all mice were returned to their home cages.

Leptin and ghrelin administration
For the leptin experiments, mice were fasted overnight. Each mouse was injected with leptin (1.5 mg/kg in 0.3 mL saline, i.p.) 30 min before the optogenetics experiment started. For MK-0667 experiments, mice were ad libitum fed. Each mouse was injected with the selective ghrelin receptor agonist, MK-0677 (1 mg/kg in 0.3 mL saline) 30 min before the optogenetics experiment started. After completion of these experiments, all caspase and control mice were provided with HFD in their home cages for 5 weeks, after which experiments were repeated.

In vivo 2-photon imaging
Multiphoton imaging was conducted with an Ultima Investigator laser scanning microscope (Bruker Nano) with a 10X air objective with 8 mm working distance and 0.5 numerical aperture (Thor Labs TL10X-2P). The 2p light source was an ALCOR 920-nm 2 W fixed wavelength laser with 100 fs pulses delivered at 80 MHz (Spark Lasers). Images were collected using resonant scanning at 30 Hz with online frame averaging, yielding 7.5 Hz (LHA) or 15 Hz (BNST) collection resolution and Prairie View software (Bruker). To activate BNST inputs to LHA, 620-nm (5 ms pulses, 3 s duration, repeated 10 times per frequency) light was delivered via an LED integrated into the light path to the lens. The PMT was shuttered during LED light pulses. The same protocol was used for imaging in control tdTomato mice. Experiments began four weeks after surgery.

For BNST imaging, male mice ($n = 4$, aged ~2 months at the time of surgery) were habituated to head fixation and trained to consume sucrose from a delivery spout. To assess activity dynamics related to satiety state, mice were either fed (free access to chow in home cage for at least 24 h prior to testing) or fasted (no access to chow in home cage for 24 h prior to testing). BNST^{Vgat}→LHA activity dynamics were recorded during consumption of 10% sucrose solution (20 trials/session). To access dynamics related to motivational state, mice ($n = 2$) were either maintained on ad libitum food and water (fed), food deprived overnight (fasted) or water deprived overnight (thirsty) prior to testing. GCaMP dynamics were then monitored in each of these three motivational states during consumption of 10% sucrose and 1% saccharine solutions (15 trials each) or 10% sucrose solution and water (15 trials each).

For LHA^{Vglut2} imaging combined with optogenetics, male mice ($n = 7$, aged 2–4 months at time of surgery) were habituated to head fixation for at least two 10-min sessions. Once mice were habituated to

the imaging setup, imaging experiments began. jGCaMP8m fluorescence from LHA^{Vglut2} somata was imaged through the GRIN lens in fed and fasted states while BNST inputs were stimulated with 620-nm light. Mice were then given ad libitum access to HFD for 3 weeks (aged 4–7 months, 27–41 g at start of HFD), and imaging was repeated. They were then placed back onto chow for three weeks before testing resumed. Fluorophore control mice expressing tdTomato in BNST projections ($n = 4$ males, aged 2 months at time of surgery) were subjected to the same fed and fasted imaging protocol as above.

Calcium imaging data acquisition, signal extraction, and analysis
Following acquisition of calcium imaging videos, data were analyzed offline using Suite2P software[76] to perform motion-correction, segmentation, and image extraction. To correct $x–y$ translations between blocks, we concatenated movies from the three imaging blocks and used Suite2P's non-rigid translation function. For BNST imaging, cell responses were aligned to the first lick after sucrose delivery (the initiation of a consummatory bout). Cells were defined as responsive via a paired t-test comparing average fluorescence in the 1-s preceding reward collection to the 1-s following the initiation of a consummatory bout ($p < 0.05$). LHA^{Vglut2} imaging data were preprocessed as above. Once fluorescent traces were extracted for each cell, LED stimulation onset as indicated by the absence of signal due to PMT shuttering was identified manually through inspection of the time-series of the mean trace of all cells and. Cell responses to stimulation were analyzed using custom Python scripts using the methodology as follows: once stimulation frames were identified, fluorescent traces were extracted for 9 s surrounding each stimulation—3 s before and after stimulation. Each cell's trace was normalized to the first 10 frames of the 9-s period. dF/F for cells in response to the stimulation was quantified for each cell by averaging the normalized fluorescence during the first 3 frames following stimulation.

Cells were tracked across imaging sessions using Suite2p-processed data. Valid ROIs were extracted, and centroid coordinates identified. The first experiment served as the baseline, with subsequent sessions aligned using a nearest-neighbor search within a predefined distance threshold. Cells with greater than 10% overlapping pixels across sessions were selected for manual validation. Automated matches were then manually evaluated for accuracy.

Brain slice electrophysiology
Vglut2-Cre mice that had been surgically injected with AAV5-hSyn-ChR2-eYFP in the BNST and AAV5-DIO-mCherry in LHA were used for LHA recording. BNST recordings were made from wild-type mice injected with retroAAV-Syn-eYFP in LHA. Recording was conducted as previously described[37]. Four to six weeks after injections, mice were deeply anesthetized with pentobarbital and then transcardially perfused with ice cold sucrose solution containing in mM: 70 sucrose, 87 NaCl, 2.5 KCl, 1.25 NaH$_2$PO$_4$, 25 NaHCO$_3$, 7 MgCl$_2$ * 6H$_2$O, 0.5 CaCl$_2$, 306–312 mOsm. Brains were rapidly removed, and coronal sections were taken through the BNST and LHA at 300 μm. Sections were incubated in artificial cerebrospinal fluid at 32 °C containing in mM: 126 NaCl, 2.5 KCl, 1.2 NaH$_2$PO$_4$, 1.2 MgCl$_2$, 26 NaHCO$_3$, 15 glucose, and 2.4 CaCl$_2$; 299–303 mOsm. Cells were visualized with a 40X objective under differential interference contrast imaging on a BX51 (Olympus) microscope. Data were acquired with an EPC 10 recording system running Patchmaster software (Heka Elektronik) at 20 kHz and bandwidth filtered with a 10 kHz Bessel filter and gain 10. Cells were excluded from all analyses if they exhibited unstable access resistance or died during recording. For HFD recordings, mice recovered from viral injection surgery for ~1 week before being switched from chow to HFD (aged 2.5–3 months, 20-29 g at HFD start). After ~3 weeks on HFD, recordings were made from fed and overnight fasted animals as above.

Current clamp recordings

Whole-cell current clamp recordings were used to validate the functionality of ChR2. Borosilicate pipettes were pulled to 4–8 MΩ and backfilled with solution containing in mM: 135 potassium gluconate, 10 HEPES, 4 KCl, 4 Mg-ATP, and 0.3, Na-GTP (pH 7.35, 285 mOsm). Current was injected to hold cells at −70 mV. eYFP+ neurons were patched within the BNST. Trains of 10 5-ms blue light pulses were delivered to the field of view at frequencies of 1–40 Hz. The spike probability was calculated for each spike train. For BNST→LHA neuron excitability recordings, eYFP-expressing BNST neurons were patched. Square pulses of current (500 ms duration, −100 to +300 pA in 20 pA steps) were injected. Evoked spikes for each step were manually counted offline in Patchmaster.

Voltage clamp recordings

Whole-cell voltage clamp recordings were used to identify LHA neurons receiving monosynaptic input from the BNST and to assess spontaneous synaptic input. Borosilicate pipettes were pulled to 4–8 MΩ and backfilled with solution containing in mM: 117 Cs-Methanesulfonate, 20 HEPES, 0.4 EGTA, 2.8 NaCl, 5 TEA, 5 Mg-ATP, and 0.5 Na-GTP (pH 7.35, 285 mOsm). Cells were held at −70 mV to evaluate EPSCs and +10 mV to evaluate IPSCs. 5 ms pulses of 470 nm light were delivered to the field of view (2 5-ms pulses spaced 100 ms apart; 10–20 sweeps of 10 s each). Spontaneous and evoked EPSCs and IPSCs were recorded. To confirm that recorded LHA neurons receive monosynaptic GABAergic input from BNST, TTX (500 nM) and 4-AP (1 mM) were applied to the external solution while eliciting optically evoked post-synaptic currents. Once monosynaptic connectivity was confirmed, gabazine (10 μM) was applied, which abolished optically evoked IPSCs. In the rare instances in which evoked EPSCs were observed in the presence of TTX, 4-AP, and gabazine, the AMPA receptor blocker DNQX (10 μM) was applied to confirm glutamatergic transmission. Paired-pulse ratio was calculated as the ratio of maximum IPSC amplitude achieved in response to the second pulse of blue light relative to the response to the first pulse. Trials in which failures occurred in response to the first pulse were excluded from analysis.

Histology

Following completion of behavioral or imaging experiments, mice were deeply anesthetized with >250 mg/kg pentobarbital (i.p.) and then transcardially perfused with ice-cold phosphate buffered saline followed by 4% paraformaldehyde. Brains were post-fixed in PFA for 24 h. Sections were taken at 35 μm with a cryostat and mounted onto microscope slides with Fluoroshield mounting medium containing DAPI (ImmunoBioScience). For NeuN staining, after incubation with blocking buffer, free floating sections were incubated in rabbit anti-NeuN primary (1:400, Millipore-Sigma ABN78) overnight at 4 degrees. They were then incubated with goat anit-rabbit 546 (1:400, Thermofisher A-11035) for two hours at room temperature, washed 3X in PBS, and mounted. Images were acquired with a Zeiss 700 confocal microscope. Minor adjustments to brightness and contrast for display purposes were made using ImageJ. For NeuN quantification, semi-automated cell counting was performed using ImageJ.

Statistical analysis

Electrophysiological data were exported from Patchmaster for offline analysis using Python to quantify evoked post-synaptic potentials. Spontaneous IPSCs and EPSCs were identified and quantified using Clampfit v11.0.3 (Molecular Devices). Statistical analyses were performed with GraphPad Prism (v10.2.1). Outliers were detected using ROUT method ($Q = 0.1\%$) and excluded from analyses. All tests were two sided and corrected for multiple comparisons and unequal variance where appropriate.

Reporting summary

Further information on research design is available in the Nature Portfolio Reporting Summary linked to this article.

Data availability

Source data are provided with this paper. The behavioral and imaging data used in this study are available at https://doi.org/10.5281/zenodo. 15133047. Source data are provided with this paper.

Code availability

Code used to analyze the data are available at https://doi.org/10.5281/ zenodo.15133047.

References

1. Malik, V. S., Willet, W. C. & Hu, F. B. Nearly a decade on—trends, risk factors and policy implications in global obesity. *Nat. Rev. Endocrinol*. **16**, 615–616 (2020).
2. Wang, Y., Beydoun, M. A., Liang, L., Caballero, B. & Kumanyika, S. K. Will all Americans become overweight or obese? estimating the progression and cost of the US obesity epidemic. *Obesity (Silver Spring)* **16**, 2323–2330 (2008).
3. Berridge, K. C., Ho, C.-Y., Richard, J. M. & DiFeliceantonio, A. G. The tempted brain eats: pleasure and desire circuits in obesity and eating disorders. *Brain Res*. **1350**, 43–64 (2010).
4. Rossi, M. A. Control of energy homeostasis by the lateral hypothalamic area. *Trends Neurosci*. **46**, 738–749 (2023).
5. Leigh, S.-J. & Morris, M. J. The role of reward circuitry and food addiction in the obesity epidemic: an update. *Biol. Psychol*. **131**, 31–42 (2018).
6. Naef, L., Pitman, K. A. & Borgland, S. L. Mesolimbic dopamine and its neuromodulators in obesity and binge eating. *CNS Spectr*. **20**, 574–583 (2015).
7. Berthoud, H.-R. & Münzberg, H. The lateral hypothalamus as integrator of metabolic and environmental needs: From electrical self-stimulation to opto-genetics. *Physiol. Behav*. **104**, 29–39 (2011).
8. Rossi, M. A. & Stuber, G. D. Overlapping brain circuits for homeostatic and hedonic feeding. *Cell Metab*. **27**, 42–56 (2018).
9. Anand, B. K. & Brobeck, J. R. Localization of a "feeding center" in the hypothalamus of the rat. *Proc. Soc. Exp. Biol. Med*. **77**, 323–325 (1951).
10. Stuber, G. D. & Wise, R. A. Lateral hypothalamic circuits for feeding and reward. *Nat. Neurosci*. **19**, 198–205 (2016).
11. Delgado, J. M. R. & Anand, B. K. Increase of food intake induced by electrical stimulation of the lateral hypothalamus. *Am. J. Physiol.-Leg. Content* **172**, 162–168 (1952).
12. Hoebel, B. G. & Teitelbaum, P. Hypothalamic control of feeding and self-stimulation. *Science* **135**, 375–377 (1962).
13. Stanley, B. G., Ha, L. H., Spears, L. C. & Dee, M. G. Lateral hypothalamic injections of glutamate, kainic acid, D,L-alpha-amino-3-hydroxy-5-methyl-isoxazole propionic acid or N-methyl-D-aspartic acid rapidly elicit intense transient eating in rats. *Brain Res*. **613**, 88–95 (1993).
14. Turenius, C. I. et al. GABA(A) receptors in the lateral hypothalamus as mediators of satiety and body weight regulation. *Brain Res*. **1262**, 16–24 (2009).
15. ANAND, B. K. & BROBECK, J. R. Hypothalamic control of food intake in rats and cats. *Yale J. Biol. Med*. **24**, 123–140 (1951).
16. Margules, D. L. & Olds, J. Identical 'feeding' and 'rewarding' systems in the lateral hypothalamus of rats. *Science* **135**, 374–375 (1962).
17. Jennings, J. H. et al. Distinct extended amygdala circuits for divergent motivational states. *Nature* **496**, 224–228 (2013).
18. Lazaridis, I. et al. A hypothalamus-habenula circuit controls aversion. *Mol. Psychiatry* **24**, 1351–1368 (2019).
19. Mickelsen, L. E. et al. Single-cell transcriptomic analysis of the lateral hypothalamic area reveals molecularly distinct populations of

inhibitory and excitatory neurons. *Nat. Neurosci.* **22**, 642–656 (2019).

20. Nieh, E. H. et al. Decoding neural circuits that control compulsive sucrose seeking. *Cell* **160**, 528–541 (2015).

21. Rossi, M. A. et al. Obesity remodels activity and transcriptional state of a lateral hypothalamic brake on feeding. *Science* **364**, 1271–1274 (2019).

22. Wang, Y. et al. EASI-FISH for thick tissue defines lateral hypothalamus spatio-molecular organization. *Cell* **184**, 6361–6377.e24 (2021).

23. Lu, Y. et al. Dorsolateral septum GLP-1R neurons regulate feeding via lateral hypothalamic projections. *Mol. Metab.* **85**, 101960 (2024).

24. Jennings, J. H., Rizzi, G., Stamatakis, A. M., Ung, R. L. & Stuber, G. D. The inhibitory circuit architecture of the lateral hypothalamus orchestrates feeding. *Science* **341**, 1517–1521 (2013).

25. Stamatakis, A. M. et al. Lateral hypothalamic area glutamatergic neurons and their projections to the lateral habenula regulate feeding and reward. *J. Neurosci.* **36**, 302–311 (2016).

26. Rossi, M. A. et al. Transcriptional and functional divergence in lateral hypothalamic glutamate neurons projecting to the lateral habenula and ventral tegmental area. *Neuron* **109**, 3823–3837.e6 (2021).

27. Fu, O. et al. Hypothalamic neuronal circuits regulating hunger-induced taste modification. *Nat. Commun.* **10**, 4560 (2019).

28. Siemian, J. N., Arenivar, M. A., Sarsfield, S. & Aponte, Y. Hypothalamic control of interoceptive hunger. *Curr. Biol.* **31**, 3797–3809.e5 (2021).

29. Walker, D. L., Toufexis, D. J. & Davis, M. Role of the bed nucleus of the stria terminalis versus the amygdala in fear, stress, and anxiety. *Eur. J. Pharmacol.* **463**, 199–216 (2003).

30. Giardino, W. J. & Pomrenze, M. B. Extended amygdala neuropeptide circuitry of emotional arousal: waking up on the wrong side of the bed nuclei of stria terminalis. *Front. Behav. Neurosci.* **15** (2021).

31. Kim, S.-Y. et al. Diverging neural pathways assemble a behavioural state from separable features in anxiety. *Nature* **496**, 219–223 (2013).

32. Giardino, W. J. et al. Parallel circuits from the bed nuclei of stria terminalis to the lateral hypothalamus drive opposing emotional states. *Nat. Neurosci.* **21**, 1084–1095 (2018).

33. Ángeles-Castellanos, M., Mendoza, J. & Escobar, C. Restricted feeding schedules phase shift daily rhythms of c-Fos and protein Per1 immunoreactivity in corticolimbic regions in rats. *Neuroscience* **144**, 344–355 (2007).

34. Kudo, T. et al. Three types of neurochemical projection from the bed nucleus of the stria terminalis to the ventral tegmental area in adult mice. *J. Neurosci.* **32**, 18035–18046 (2012).

35. Li, H. E. et al. Hypothalamic-extended amygdala circuit regulates temporal discounting. *J. Neurosci.* **41**, 1928–1940 (2021).

36. Wang, Y. et al. A bed nucleus of stria terminalis microcircuit regulating inflammation-associated modulation of feeding. *Nat. Commun.* **10**, 2769 (2019).

37. Shrivastava, K. et al. Maternal overnutrition is associated with altered synaptic input to lateral hypothalamic area. *Mol. Metab.* **71**, 101702 (2023).

38. Fenno, L. E. et al. Comprehensive dual- and triple-feature intersectional single-vector delivery of diverse functional payloads to cells of behaving mammals. *Neuron* **107**, 836–853.e11 (2020).

39. Otis, J. M. et al. Paraventricular thalamus projection neurons integrate cortical and hypothalamic signals for cue-reward processing. *Neuron* **103**, 423–431.e4 (2019).

40. K Namboodiri, V. M. et al. Relative salience signaling within a thalamo-orbitofrontal circuit governs learning rate. *Curr. Biol.* **31**, 5176–5191.e5 (2021).

41. Yang, C. F. et al. Sexually dimorphic neurons in the ventromedial hypothalamus govern mating in both sexes and aggression in males. *Cell* **153**, 896–909 (2013).

42. Gray, D. C., Mahrus, S. & Wells, J. A. Activation of specific apoptotic caspases with an engineered small-molecule-activated protease. *Cell* **142**, 637–646 (2010).

43. Olszewski, P. K. et al. Neural basis of orexigenic effects of ghrelin acting within lateral hypothalamus. *Peptides* **24**, 597–602 (2003).

44. Leinninger, G. M. et al. Leptin acts via leptin receptor-expressing lateral hypothalamic neurons to modulate the mesolimbic dopamine system and suppress feeding. *Cell Metab.* **10**, 89–98 (2009).

45. Bagnasco, M., Kalra, P. S. & Kalra, S. P. Ghrelin and leptin pulse discharge in fed and fasted rats. *Endocrinology* **143**, 726–729 (2002).

46. Weigle, D. S. et al. Effect of fasting, refeeding, and dietary fat restriction on plasma leptin levels*. *J. Clin. Endocrinol. Metab.* **82**, 561–565 (1997).

47. Ahima, R. S. et al. Role of leptin in the neuroendocrine response to fasting. *Nature* **382**, 250–252 (1996).

48. Fritz, E. M., Pierre, A., De Bundel, D. & Singewald, N. Ghrelin receptor agonist MK0677 and overnight fasting do not rescue deficient fear extinction in 129S1/SvImJ mice. *Front. Psychiatry* **14** (2023).

49. Garcia, A. et al. Lateral hypothalamic GABAergic neurons encode and potentiate sucrose's palatability. *Front Neurosci.* **14**, 608047 (2021).

50. Lee, Y. H. et al. Lateral hypothalamic leptin receptor neurons drive hunger-gated food-seeking and consummatory behaviours in male mice. *Nat. Commun.* **14**, 1486 (2023).

51. Petzold, A., van den Munkhof, H. E., Figge-Schlensok, R. & Korotkova, T. Complementary lateral hypothalamic populations resist hunger pressure to balance nutritional and social needs. *Cell Metab.* **35**, 456–471.e6 (2023).

52. Al Massadi, O., López, M., Tschöp, M., Diéguez, C. & Nogueiras, R. Current understanding of the hypothalamic ghrelin pathways inducing appetite and adiposity. *Trends Neurosci.* **40**, 167–180 (2017).

53. Mani, B. K. et al. The role of ghrelin-responsive mediobasal hypothalamic neurons in mediating feeding responses to fasting. *Mol. Metab.* **6**, 882–896 (2017).

54. Mazzone, C. M. et al. High-fat food biases hypothalamic and mesolimbic expression of consummatory drives. *Nat. Neurosci.* **23**, 1253-1266 (2020).

55. Beutler, L. R. et al. Obesity causes selective and long-lasting desensitization of AgRP neurons to dietary fat. *eLife* **9**, e55909 (2020).

56. Cummings, D. E. et al. A preprandial rise in plasma ghrelin levels suggests a role in meal initiation in humans. *Diabetes* **50**, 1714–1719 (2001).

57. la Fleur, S. E. et al. A reciprocal interaction between food-motivated behavior and diet-induced obesity. *Int J. Obes.* **31**, 1286–1294 (2007).

58. Sharma, S. & Fulton, S. Diet-induced obesity promotes depressive-like behaviour that is associated with neural adaptations in brain reward circuitry. *Int J. Obes.* **37**, 382–389 (2013).

59. Tracy, A. L., Wee, C. J. M., Hazeltine, G. E. & Carter, R. A. Characterization of attenuated food motivation in high-fat diet-induced obesity: critical roles for time on diet and reinforcer familiarity. *Physiol. Behav.* **141**, 69–77 (2015).

60. Rabasa, C. et al. Behavioral consequences of exposure to a high fat diet during the post-weaning period in rats. *Hormones Behav.* **85**, 56–66 (2016).

61. Arcego, D. M. et al. Chronic high-fat diet affects food-motivated behavior and hedonic systems in the nucleus accumbens of male rats. *Appetite* **153**, 104739 (2020).

62. Stice, E., Spoor, S., Bohon, C., Veldhuizen, M. G. & Small, D. M. Relation of reward from food intake and anticipated food intake to obesity: a functional magnetic resonance imaging study. *J. Abnorm. Psychol.* **117**, 924–935 (2008).

63. Stice, E., Spoor, S., Bohon, C. & Small, D. M. Relation between obesity and blunted striatal response to food is moderated by TaqIA A1 Allele. *Science* **322**, 449–452 (2008).

64. Wang, G.-J. et al. Brain dopamine and obesity. *Lancet* **357**, 354–357 (2001).

65. Small, D. M. Individual differences in the neurophysiology of reward and the obesity epidemic. *Int J. Obes.* **33**, S44–S48 (2009).

66. Sheng, H. et al. Nucleus accumbens circuit disinhibits lateral hypothalamus glutamatergic neurons contributing to morphine withdrawal memory in male mice. *Nat. Commun.* **14**, 71 (2023).

67. Takahashi, K. A. & Cone, R. D. Fasting induces a large, leptin-dependent increase in the intrinsic action potential frequency of orexigenic arcuate nucleus neuropeptide Y/Agouti-related protein neurons. *Endocrinology* **146**, 1043–1047 (2005).

68. Liu, T. et al. Fasting activation of AgRP neurons requires NMDA receptors and involves spinogenesis and increased excitatory tone. *Neuron* **73**, 511–522 (2012).

69. Li, G. et al. Brain functional and structural magnetic resonance imaging of obesity and weight loss interventions. *Mol. Psychiatry* **28**, 1466–1479 (2023).

70. Haltia, L. T. et al. Brain white matter expansion in human obesity and the recovering effect of dieting. *J. Clin. Endocrinol. Metab.* **92**, 3278–3284 (2007).

71. Frank, S. et al. Altered brain activity in severely obese women may recover after Roux-en Y gastric bypass surgery. *Int J. Obes.* **38**, 341–348 (2014).

72. Nieh, E. H. et al. Inhibitory input from the lateral hypothalamus to the ventral tegmental area disinhibits dopamine neurons and pro-motes behavioral activation. *Neuron* **90**, 1286–1298 (2016).

73. Rodriguez-Romaguera, J. et al. Prepronociceptin-expressing neu-rons in the extended amygdala encode and promote rapid arousal responses to motivationally salient stimuli. *Cell Rep.* **33** (2020).

74. Vong, L. et al. Leptin action on GABAergic neurons prevents obesity and reduces inhibitory tone to POMC neurons. *Neuron* **71**, 142–154 (2011).

75. Fenno, L. E. et al. Targeting cells with single vectors using multiple-feature Boolean logic. *Nat. Methods* **11**, 763–772 (2014).

76. Pachitariu, M. et al. Suite2p: beyond 10,000 neurons with standard two-photon microscopy. *bioRxiv* https://doi.org/10.1101/061507 (2017).

Acknowledgements

Author contributions

Conceptualization: M.A.R. and K.S., Methodology: M.A.R., K.S. and V.A., Investigation: M.A.R., K.S., V.A., Y.L., A.H., J.L. and T.K., Visualization: M.A.R., K.S., V.A. Y.L. and J.L., Supervision: M.A.R., Writing—original draft: M.A.R. and K.S., Writing—review & editing: M.A.R., K.S., V.A., Y.L., J.L., A.H. and T.K.

Competing interests

The authors declare no competing interests.

Additional information

Supplementary information The online version contains supplementary material available at https://doi.org/10.1038/s41467-025-59686-2.

Correspondence and requests for materials should be addressed to Mark A. Rossi.

Peer review information *Nature Communications* thanks William Giardino, who co-reviewed with Faith Aloboudi and the other, anonymous, reviewer(s) for their contribution to the peer review of this work. A peer review file is available.

Reprints and permissions information is available at http://www.nature.com/reprints

Publisher's note Springer Nature remains neutral with regard to jurisdictional claims in published maps and institutional affiliations.